LNGS/exp-01/02
5 Jun 02

Status Report of the MACRO Experiment for the year 2001

MACRO Collaboration

M. Ambrosio[12], R. Antolini[7], G. Auriemma[14,a], D. Bakari[2,17], A. Baldini[13], G. C. Barbarino[12], B. C. Barish[4], G. Battistoni[6,b], Y. Becherini[2], R. Bellotti[1], C. Bemporad[13], P. Bernardini[10], H. Bilokon[6], C. Bloise[6], C. Bower[8], M. Brigida[1], S. Bussino[18], F. Cafagna[1], M. Calicchio[1], D. Campana[12], M. Carboni[6], R. Caruso[9], S. Cecchini[2,c], F. Cei[13], V. Chiarella[6], B. C. Choudhary[4], S. Coutu[11,i], M. Cozzi[2], G. De Cataldo[1], H. Dekhissi[2,17], C. De Marzo[1], I. De Mitri[10], J. Derkaoui[2,17], M. De Vincenzi[18], A. Di Credico[7], O. Erriquez[1], C. Favuzzi[1], C. Forti[6], P. Fusco[1], G. Giacomelli[2], G. Giannini[13,d], N. Giglietto[1], M. Giorgini[2], M. Grassi[13], L. Gray[7], A. Grillo[7], F. Guarino[12], C. Gustavino[7], A. Habig[3,p], K. Hanson[11], R. Heinz[8], E. Iarocci[6,e], E. Katsavounidis[4,q], I. Katsavounidis[4,r], E. Kearns[3], H. Kim[4], S. Kyriazopoulou[4], E. Lamanna[14,l], C. Lane[5], D. S. Levin[11], P. Lipari[14], N. P. Longley[4,h], M. J. Longo[11], F. Loparco[1], F. Maaroufi[2,17], G. Mancarella[10], G. Mandrioli[2], S. Manzoor[2,n], A. Margiotta[2], A. Marini[6], D. Martello[10], A. Marzari-Chiesa[16], P. Matteuzzi[2], M. N. Mazziotta[1], D. G. Michael[4], S. Mikheyev[4,7,f], L. Miller[8,m], P. Monacelli[9], T. Montaruli[1], M. Monteno[16], S. Mufson[8], J. Musser[8], D. Nicolò[13], R. Nolty[4], C. Orth[3], G. Osteria[12], O. Palamara[7], V. Patera[6,e], L. Patrizii[2], R. Pazzi[13], C. W. Peck[4], L. Perrone[10], S. Petrera[9], P. Pistilli[18], V. Popa[2,g], A. Rainò[1], J. Reynoldson[7], F. Ronga[6], A. Rrhioua[2,17], C. Satriano[14,a], E. Scapparone[7], K. Scholberg[3,q], A. Sciubba[6,e], P. Serra[2], M. Sioli[2], G. Sirri[2], M. Sitta[16,o], P. Spinelli[1], M. Spinetti[6], M. Spurio[2], R. Steinberg[5], J. L. Stone[3], L. R. Sulak[3], A. Surdo[10], G. Tarlè [11], V. Togo[2], M. Vakili[15,s], C. W. Walter[3,4], and R. Webb[15].

[1] *Dipartimento di Fisica dell'Università di Bari and INFN, 70126 Bari, Italy*
[2] *Dipartimento di Fisica dell'Università di Bologna and INFN, 40126 Bologna, Italy*
[3] *Physics Department, Boston University, Boston, MA 02215, USA*
[4] *California Institute of Technology, Pasadena, CA 91125, USA*
[5] *Department of Physics, Drexel University, Philadelphia, PA 19104, USA*
[6] *Laboratori Nazionali di Frascati dell'INFN, 00044 Frascati (Roma), Italy*
[7] *Laboratori Nazionali del Gran Sasso dell'INFN, 67010 Assergi (L'Aquila), Italy*
[8] *Depts. of Physics and of Astronomy, Indiana University, Bloomington, IN 47405, USA*
[9] *Dipartimento di Fisica dell'Università dell'Aquila and INFN, 67100 L'Aquila, Italy*
[10] *Dipartimento di Fisica dell'Università di Lecce and INFN, 73100 Lecce, Italy*
[11] *Department of Physics, University of Michigan, Ann Arbor, MI 48109, USA*
[12] *Dipartimento di Fisica dell'Università di Napoli and INFN, 80125 Napoli, Italy*
[13] *Dipartimento di Fisica dell'Università di Pisa and INFN, 56010 Pisa, Italy*
[14] *Dipartimento di Fisica dell'Università di Roma "La Sapienza" and INFN, 00185 Roma, Italy*
[15] *Physics Department, Texas A&M University, College Station, TX 77843, USA*

[16] *Dipartimento di Fisica Sperimentale dell'Università di Torino and INFN, 10125 Torino, Italy*
[17] *L.P.T.P., Faculty of Sciences, University Mohamed I, B.P. 524 Oujda, Morocco*
[18] *Dipartimento di Fisica dell'Università di Roma Tre and INFN Sezione Roma Tre, 00146 Roma, Italy*
[a] *Also Università della Basilicata, 85100 Potenza, Italy*
[b] *Also INFN Milano, 20133 Milano, Italy*
[c] *Also Istituto TESRE/CNR, 40129 Bologna, Italy*
[d] *Also Università di Trieste and INFN, 34100 Trieste, Italy*
[e] *Also Dipartimento di Energetica, Università di Roma, 00185 Roma, Italy*
[f] *Also Institute for Nuclear Research, Russian Academy of Science, 117312 Moscow, Russia*
[g] *Also Institute for Space Sciences, 76900 Bucharest, Romania*
[h] *Also Macalester College, Dept. of Physics and Astr., St. Paul, MN 55105* [i] *Also Department of Physics, Pennsylvania State University, University Park, PA 16801, USA*
[l] *Also Dipartimento di Fisica dell'Università della Calabria, Rende (Cosenza), Italy*
[m] *Also Department of Physics, James Madison University, Harrisonburg, VA 22807, USA*
[n] *Also RPD, PINSTECH, P.O. Nilore, Islamabad, Pakistan*
[o] *Also Dipartimento di Scienze e Tecnologie Avanzate, Università del Piemonte Orientale, Alessandria, Italy*
[p] *Also U. Minn. Duluth Physics Dept., Duluth, MN 55812*
[q] *Also Dept. of Physics, MIT, Cambridge, MA 02139*
[r] *Also Intervideo Inc., Torrance CA 90505 USA*
[s] *Also Resonance Photonics, Markham, Ontario, Canada*

Abstract

In this 2001 status report of the MACRO experiment, results are presented on atmospheric neutrinos and neutrino oscillations, high energy neutrino astronomy, searches for WIMPs, search for low energy stellar gravitational collapse neutrinos, stringent upper limits on GUT magnetic monopoles, nuclearites and lightly ionizing particles, high energy downgoing muons, primary cosmic ray composition and shadowing of primary cosmic rays by the Moon and the Sun.

1 Introduction

MACRO was a large area multipurpose underground detector designed to search for rare events in the cosmic radiation. It was optimized to look for the supermassive magnetic monopoles predicted by Grand Unified Theories (GUT) of the electroweak and strong interactions; it could also perform measurements in areas of astrophysics, nuclear, particle and cosmic ray physics. These include the study of atmospheric neutrinos and neutrino oscillations, high energy ($E_\nu \gtrsim 1$ GeV) neutrino astronomy, indirect searches for WIMPs, search for low energy ($E_\nu \gtrsim 7$ MeV) stellar collapse neutrinos, studies of various aspects of the high energy underground muon flux (which is an indirect tool to study the primary cosmic ray composition, origin and interactions), searches for fractionally charged particles and other rare particles that may exist in the cosmic radiation.

The mean rock depth of the overburden is $\simeq 3700$ m.w.e., while the minimum is 3150 m.w.e. This defines the minimum muon energy at the surface at ~ 1.3 TeV in order to reach MACRO. The average residual energy and the muon flux at the MACRO depth are ~ 320 GeV and $\sim 1\,\mathrm{m}^{-2}\mathrm{h}^{-1}$, respectively.

The detector was built and equipped with electronics during the years $1988-1995$. It started data taking with part of the apparatus in 1989; it was completed in 1995 and it was running in its final configuration until December 19, 2000. It may be worth pointing out that all the physics and astrophysics items proposed in the 1984 Proposal were covered and good results were obtained on each of them, even beyond the most rosy anticipations.

The highlights of the new results have been presented at the 2001 summer conferences (in particular at the Int. Cosmic Ray Conf. (ICRC) in Hamburg, at the 2001 European HEP in Budapest, at TAUP 2001 at Gran Sasso and at the NATO Advanced Research Workshop in Oujda, Morocco). One of the main results is the evidence for anomalies in the atmospheric ν_μ flux, which are well interpreted in terms of $\nu_\mu \to \nu_\tau$ oscillations.

We shall give a short summary of the detector and of its performances; this will be followed by an overview of the main physics and astrophysics results obtained by MACRO. A complete list of MACRO papers is given in [1]-[36]; other information may be found in http://www.df.unibo.it/macro/pub1.htm.

In the year 2001 four papers were published on refereed journals; they concerned high energy neutrino astronomy with the MACRO detector [33], the preference for $\nu_\mu \to \nu_\tau$ oscillations over $\nu_\mu \to \nu_s$ [34], a technical paper on the MACRO detector [35] and a combined analysis for a search for magnetic monopoles [36]. Several results appeared in preliminary form in 14 paper contributions that were published in various physics conference proceedings [37]-[64]. They concerned the study of high and low energy atmospheric neutrinos, the use of multiple Coulomb scattering for determining neutrino energies, high energy muon neutrino astronomy, several rare particle searches, the observation of the moon and sun shadow of high energy primary cosmic rays and several aspects of "muon astronomy".

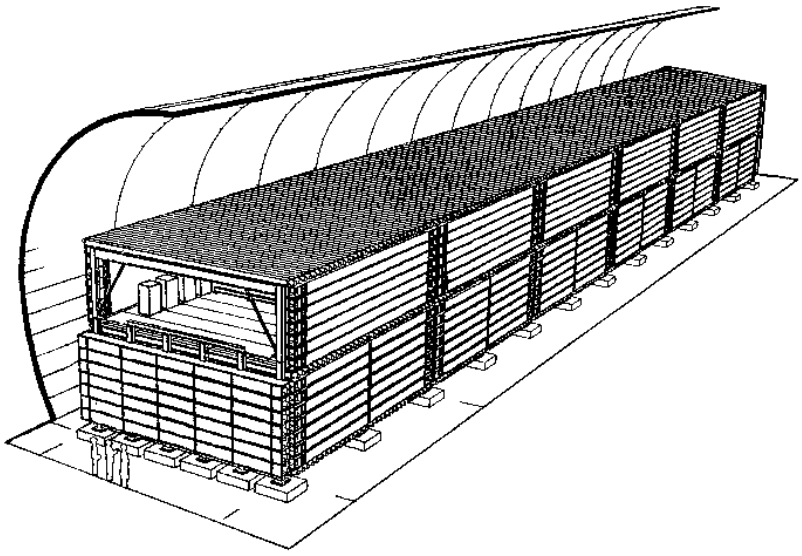

Figure 1: General layout of the MACRO detector which was installed in Hall B of the LNGS. Overall dimensions of the active part were $76.5 \times 12 \times 9.3$ m^3. [35]

2 The Detector

The MACRO detector had a modular structure: it was divided into six sections referred to as supermodules. Each active part of one supermodule had a size of $12.6 \times 12 \times 9.3\,\mathrm{m}^3$ and had a separate mechanical structure and electronics readout. The full detector had global dimensions of $76.5 \times 12 \times 9.3\,\mathrm{m}^3$ and provided a total acceptance to an isotropic flux of particles of $\sim 10,000\,\mathrm{m}^2\,\mathrm{sr}$. The total mass was $\simeq 5300$ t.

Redundancy and complementarity have been the primary goals in designing the experiment. Since no more than few magnetic monopoles could be expected, multiple signatures and ability to perform cross checks among various parts of the apparatus were important.

The detector was composed of three sub-detectors: liquid scintillation counters, limited streamer tubes and nuclear track detectors. Each one of them could be used in "stand-alone" and in "combined" mode. A general layout of the experiment is shown in Fig. 1. Notice the division in the *lower* MACRO and in the *upper* part, often referred to as the *Attico*; the inner part of the *Attico* was empty and lodged the electronics. The mass of the *lower* MACRO was $\simeq 4200$ t, mainly in the form of boxes filled with crushed Gran Sasso rock. Fig. 2 shows a cross section of the apparatus.

The scintillation subdetector. Each supermodule contained 77 scintillation counters, divided into three horizontal planes (bottom, center, and top) and two vertical planes (east and west). In the lower part, the bottom and center horizontal planes had 16 scintillation counters, the east and west vertical planes had 7 counters each. In the *Attico*, the top plane had 17 scintillation counters, the east and west vertical planes had 7 counters

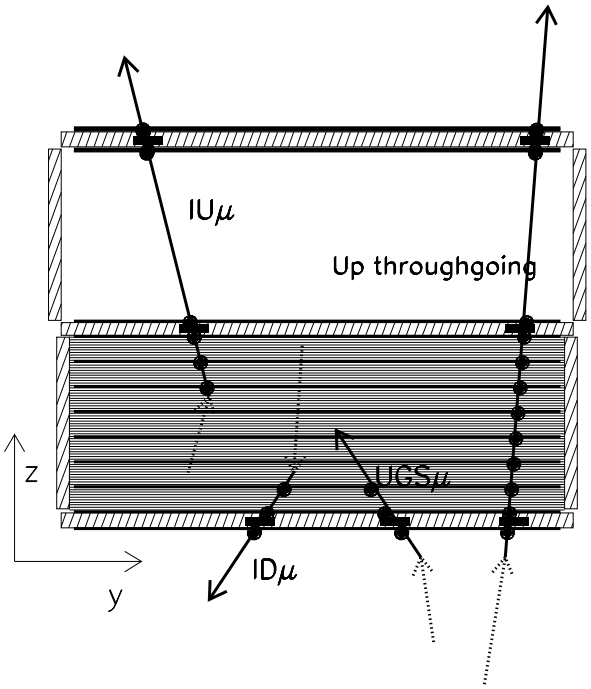

Figure 2: Vertical cross section of the detector and sketch of different event topologies induced by ν_μ interactions in or around MACRO. The black points and the black rectangles represent streamer tubes and scintillator hits, respectively. Tracking was performed by the streamer tubes; the time-of-flight of the muons was measured by the scintillators for *Up Semicontained* (Internal upgoing - IU μ) and *Upthroughgoing* events (and also for downgoing muons).

each. The lower part of the north and south faces of the detector were covered by vertical walls with seven scintillation counters each. The upper parts of these faces were left open in order to allow access to the readout electronics.

The active volume of each horizontal scintillation counter was $11.2 \times 0.73 \times 0.19\,\mathrm{m}^3$, while for the vertical ones it was $11.1 \times 0.22 \times 0.46\,\mathrm{m}^3$. All scintillator boxes were filled with a mixture of high purity mineral oil (96.4 %) and pseudocumene (3.6 %), with an additional 1.44 g/l of PPO and 1.44 mg/l of bis-MSB as wavelength shifters. The horizontal counters were seen by two 8″ photomultipliers (PMTs) and the vertical counters by one 8″ PMT at each end. Each PMT housing was equipped with a light collecting mirror. The total number of scintillators was 476 (294 horizontal and 182 vertical) with a total active mass of almost 600 tons. Minimum ionizing muons when crossing vertically the 19 cm of scintillator in a counter release an average energy of $\simeq 34$ MeV and were measured with a timing and longitudinal position resolution of $\simeq 500$ ps and $\simeq 10$ cm, respectively.

The scintillation counters were equipped with specific triggers for rare particles, muons and low energy neutrinos from stellar gravitational collapses. The Slow Monopole Trigger (SMT) was sensitive to magnetic monopoles with velocities from about $10^{-4}c$ to $10^{-2}c$, the Fast Monopole Trigger (FMT) was sensitive to monopoles with velocities from about $5 \times 10^{-3}c$ to $5 \times 10^{-2}c$, the Lightly Ionizing Particle trigger was sensitive to fractionally charged particles, the Energy Reconstruction Processor (ERP) and "CSPAM" were primarily muon triggers (but used also for relativistic monopoles) and the gravitational collapse neutrino triggers (the Pulse Height Recorder and Synchronous Encoder –PHRASE– and

the ERP) were optimized to trigger on bursts of low energy events in the liquid scintillator. The scintillator system was complemented by a 200 MHz waveform digitizing (WFD) system used in rare particle searches, and in any occasion where knowledge of the PMT waveform was useful.

The streamer tube subsystem. *The lower part* of the detector contained ten horizontal planes of limited streamer tubes, the middle eight of which were interleaved by seven rock absorbers (total thickness $\simeq 360\,\mathrm{g\,cm^{-2}}$). This sets a $\simeq 1$ GeV energy threshold for muons vertically crossing the lower part of the detector. At the top of the *Attico* there were four horizontal streamer tube planes, two above and two below the top scintillator layer. On each lateral wall six streamer tube planes sandwiched the corresponding vertical scintillator plane (three streamer planes on each side). Each tube had a $3 \times 3\,\mathrm{cm^2}$ cross section and was 12 m long. The total number of tubes was 50304, all filled with a gas mixture of He (73 %) and n-pentane (27 %). They were equipped with 100μ *Cu/Be* wires and stereo pickup strips at an angle of 26.5°. The tracking resolution of the streamer tube system was $\simeq 1$ cm, corresponding to an angular accuracy of $\simeq 0.2°$ over the 9.3 m height of MACRO. The real angular resolution was limited to $\simeq 1°$ by the multiple Coulomb scattering of muons in the rock above the detector. The streamer tubes were read by 8-channel cards (one channel for each wire) which discriminated the signals and sent the analog information (time development and total charge) to an ADC/TDC system (the QTP). The signals were used to form two different chains (Fast and Slow) of TTL pulses, which were the inputs for the streamer tube Fast and Slow Particle Triggers. In the 11 years of operation only 50 wires were lost.

The nuclear track subdetector was deployed in three planes, horizontally in the center of the lower section and vertically on the East and North faces. The detector was divided in 18126 modules, which could be individually extracted and substituted. Each module ($\sim 24.5 \times 24.5 \times 0.65\,\mathrm{cm^3}$) was composed of three layers of CR39, three layers of Lexan and 1 mm Aluminium absorber to stop nuclear fragments.

The Transition Radiation Detector (TRD). A TRD was installed in part of the *Attico*, right above the central horizontal scintillator plane of the main detector. It was composed of three individual modules (overall dimensions $6 \times 6 \times 2\,\mathrm{m^3}$) and it was made of 10 cm thick polyethylene foam radiators and proportional counters; each counter measured $6 \times 6 \times 600\,\mathrm{cm^3}$ and was filled with Ar (90 %) and CO_2 (10 %). The TRD provided a measurement of the muon energy in the range of $100\,\mathrm{GeV} < E < 930\,\mathrm{GeV}$; muons of higher energies could also be detected and counted.

Fig. 3 shows four photographs of the Hall B taken from its south side: (a) 1987: before starting construction; (b) 1990: the 1st lower supermodule was taking data, while the second and the third were under construction; (c) the full MACRO detector in 1995 (a safety stairs and a ventilation system were added later in front of the apparatus); (d) Hall B empty again in 2001. (You can find the pictures at this address: http://www.df.unibo.it/margiotta/rep_01/ with the names: fig3a.eps, fig3b.eps, fig3c.eps, fig3d.eps.)

Fig. 4 shows a "group" of 11 downgoing muons as seen in the lateral view (wire view) by the MACRO Event Display (which also included a strip view and side views).

(a) (b)

(c) (d)

Figure 3: Photographs of Hall B taken from its south side: (a) In 1987 just before starting construction; (b) in 1990 when the first lower supermodule was taking data while the second and the third were under construction; (c) in 1995 when the completed MACRO detector started data taking (notice that safety stairs and a ventilation system were added later in front of the apparatus; (d) Hall B empty in 2001. (You can find the pictures at this address: http://www.df.unibo.it/margiotta/rep_01/ with the names: fig3a.eps, fig3b.eps, fig3c.eps, fig3d.eps.)

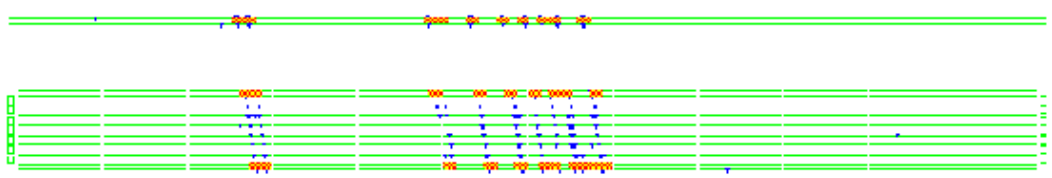

Figure 4: MACRO Event Display. A group of 11 downgoing muons as observed by part of the lateral view.

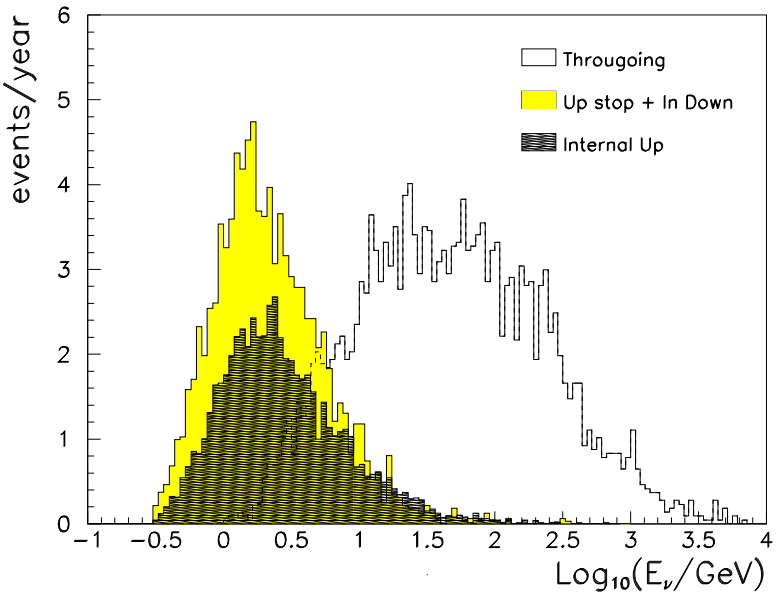

Figure 5: Distributions of the parent muon neutrino energies giving rise to the different event topologies, upthroughgoing, upsemicontained and upstopping plus downsemicontained, with median neutrino energies of approximately 50, 4.2 and 3.5 GeV, respectively.

3 Atmospheric neutrino oscillations

Upward going muons are identified using the streamer tube system (for tracking) and the scintillator system (for time-of-flight measurement). A rejection factor of at least 10^7 is needed, and was reached, in order to separate upgoing muons from the background due to the downgoing muons. Fig. 2 shows a sketch of the different neutrino event topologies analyzed: Upthroughgoing muons, Upsemicontained (also called Internal Upgoing muons, IU), Upgoing Stopping muons (UGS), Internal Downgoing muons (ID). Fig. 5 shows the parent ν_μ energy spectra for the three event topologies, computed by Monte Carlo methods. The number of events measured and expected for the three topologies are given in Table 1. All the data samples deviate from the MC expectations; the deviations point out to the same $\nu_\mu \rightarrow \nu_\tau$ oscillation scenario.

The background on upgoing muons arising from downgoing muons interacting in the rock around MACRO and giving an upward going charged particle was studied in detail for upthroughgoing muons in [24]. The selection cuts reduce this background to $< 1\%$.

3.1 Upthroughgoing muons

The *upthroughgoing muons* come from ν_μ interactions in the rock below the detector; the ν_μ's have a median energy $\overline{E}_\nu \sim$ 50 GeV. The upthroughgoing muons with $E_\mu > 1\,\mathrm{GeV}$ cross the whole detector. The time information provided by the scintillation counters allows the determination of the direction (versus) by the time-of-flight (T.o.F.) method. The data of Fig. 6 refer to the running period 3/1989 - 4/1994 with the detector under

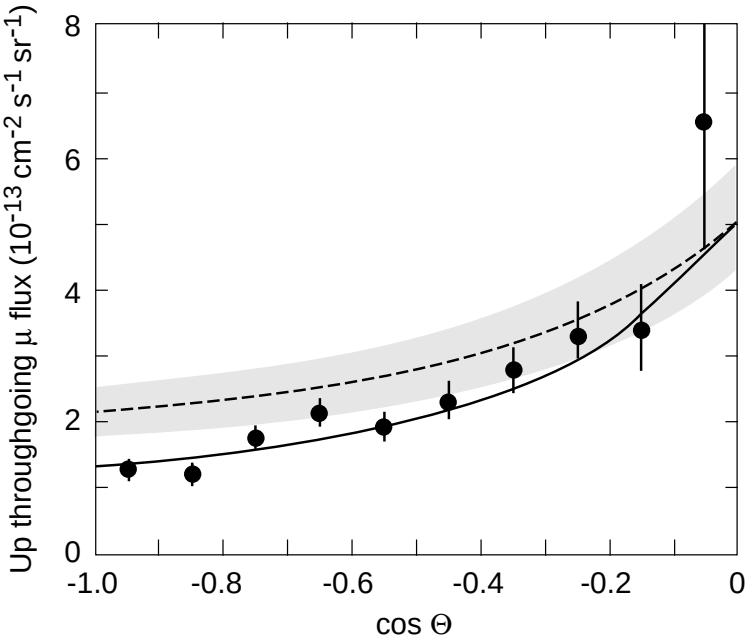

Figure 6: Zenith angle distribution of upthroughgoing muons (black points). The dashed line is the expectation for no oscillations (with a 17 % scale uncertainty band). The solid line is the fit for an oscillated muon flux with maximum mixing and $\Delta m^2 = 2.5 \cdot 10^{-3}$ eV^2.

construction, and with the full detector till 12/2000; the total livetime was 6.16 years (full detector equivalent) [17, 25, 47, 54]. The data deviate in absolute value and in shape from the MC predictions. This was first pointed at TAUP 1993 and in [17] in 1995.

We studied a large number of possible systematic effects that could affect our measurements: no significant systematic problems exist in the detector or in the data analyses. One of the most significant checks was performed using only the scintillator system with the PHRASE Wave Form Digitizers, completely independent of the ERP system.

The measured data have been compared with Monte Carlo simulations. For the upthroughgoing muon simulation, the neutrino flux computed by the Bartol group is used [65]. The cross sections for the neutrino interactions were calculated using the deep inelastic parton distributions of ref. [66] The muon propagation to the detector was done using the energy loss calculation in standard rock [67]. The total systematic uncertainty on the expected muon flux, obtained adding in quadrature the errors from neutrino flux, cross section and muon propagation, is estimated to be 17 %. This uncertainty is mainly a scale error; the error on the shape of the angular distribution is $\sim 5\%$. Fig. 6 shows the zenith angle distribution of the measured flux of upthroughgoing muons. The Monte Carlo expectation for no oscillations is shown as a dashed line.

To test the oscillation hypothesis, the independent probabilities for obtaining the observed number of events and the shape of the angular distribution have been calculated for various parameter values. The value of Δm^2 obtained from the shape of the angular distribution is equal to the value obtained from the observed reduction in the number of events. For $\nu_\mu \rightarrow \nu_\tau$ oscillations, combining the probabilities from the two independent tests on the shape of the zenith angle distribution and on the total number of events, the

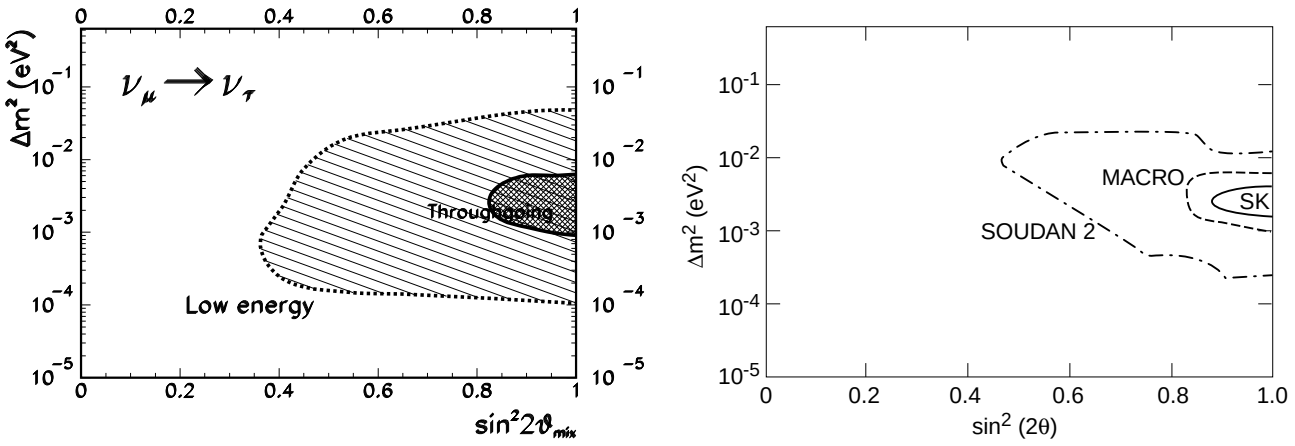

(a) (b)

Figure 7: (a) Allowed regions, at 90 % c.l., for $\nu_\mu \rightarrow \nu_\tau$ oscillations from the MACRO upthroughgoing muon sample and from the low energy events. (b) Comparison with the Soudan 2 [71] and SuperK [70] allowed regions.

maximum probability is 66%; the best parameters are $\Delta m^2 = 2.5 \cdot 10^{-3}$ eV^2 and maximal mixing; the result of the fit is the solid line in Fig. 6. The probability for no-oscillations is 0.4 %.

Fig. 7a shows the allowed regions for the $\nu_\mu \rightarrow \nu_\tau$ oscillation parameters in the $sin^2 2\theta - \Delta m^2$ plane, computed according to ref. [68] for the upthroughgoing muons and for the low energy events. The MACRO 90% c.l. allowed region for $\nu_\mu \rightarrow \nu_\tau$ is compared in Fig. 7b with those obtained by the SuperKamiokande (SK) [70] and Soudan 2 experiments [71].

3.2 Matter effects. $\nu_\mu \rightarrow \nu_\tau$ against $\nu_\mu \rightarrow \nu_{sterile}$

Matter effects due to the difference between the weak interaction effective potential for muon neutrinos with respect to sterile neutrinos (which have null potential) would produce a different total number and a different zenith distribution of upthroughgoing muons [34].

In Fig. 8 the measured ratio between the events with $-1 < cos\theta < -0.7$ and the events with $-0.4 < cos\theta < 0$ is shown as a black point. In this ratio most of the theoretical uncertainties on neutrino flux and cross section cancel. The remaining theoretical error is estimated at $\leq 5\%$. The systematic experimental error on the ratio, due to analysis cuts and detector efficiencies, is 4.6%. Combining the experimental and theoretical errors in quadrature, a global estimate of 7% is obtained. MACRO measured 305 events with $-1 < cos\theta < -0.7$ and 206 with $-0.4 < cos\theta < 0$; the ratio is $\mathrm{R} = 1.48 \pm 0.13_{stat} \pm 0.10_{sys}$. For $\Delta m^2 = 2.5 \cdot 10^{-3}$ eV^2 and maximal mixing, the minimum expected value of the ratio for $\nu_\mu \rightarrow \nu_\tau$ is $R_\tau = 1.72$ while for $\nu_\mu \rightarrow \nu_s$ is $R_{sterile} = 2.16$. The maximum probabilities P_{best} to find a value of R_τ and of $R_{sterile}$ smaller than the expected ones are 9.4 % and 0.06

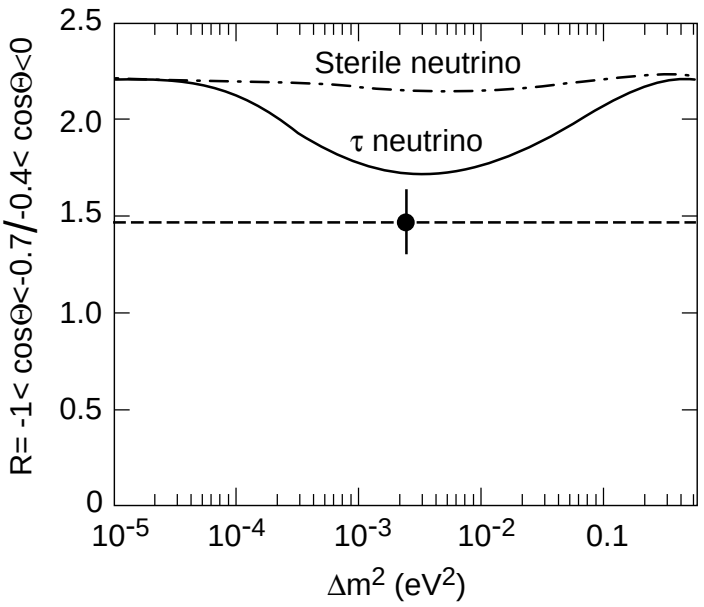

Figure 8: Ratio of events with $-1 < cos\theta < -0.7$ to events with $-0.4 < cos\theta < 0$ as a function of Δm^2 for maximal mixing. The black point with error bar is the measured value, the solid line is the prediction for $\nu_\mu \to \nu_\tau$ oscillations, the dash-dotted line is the prediction for $\nu_\mu \to \nu_{sterile}$ oscillations.

% respectively. Hence the ratio of the maximum probabilities is $P_{best_\tau}/P_{best_{sterile}} = 157$, so that $\nu_\mu \to \nu_s$ oscillations are disfavoured at 99% c.l. compared to the $\nu_\mu \to \nu_\tau$ channel with maximal mixing and $\Delta m^2 = 2.5 \cdot 10^{-3}$ eV^2.

3.3 ν_μ energy estimates by multiple Coulomb scattering of upthroughgoing muons

The oscillation probability is a function of the ratio L/E_ν. E_ν may be estimated by measuring the muon energy E_μ, which was done using their Multiple Coulomb Scattering (MCS) in the absorbers.

The r.m.s. of the lateral displacement for a muon crossing the whole apparatus on the vertical is $\sigma_{MCS} \simeq 10\,\mathrm{cm/E_\mu(\,GeV)}$. The muon energy E_μ estimate can be performed up to a saturation point, occurring when σ_{MCS} is comparable with the detector space resolution.

Two MCS analyses were performed.

The first analysis was made studying the deflection of upthroughgoing muons with the streamer tubes in digital mode. Using MC methods to estimate the muon energy from its scattering angle, the data were divided into 3 subsamples with different average energies, in 2 samples in zenith angle θ and finally in 5 subsamples with different average values of L/E_ν. This method could reach a spatial resolution of $\sim 1\,\mathrm{cm}$; it yielded an L/E_ν

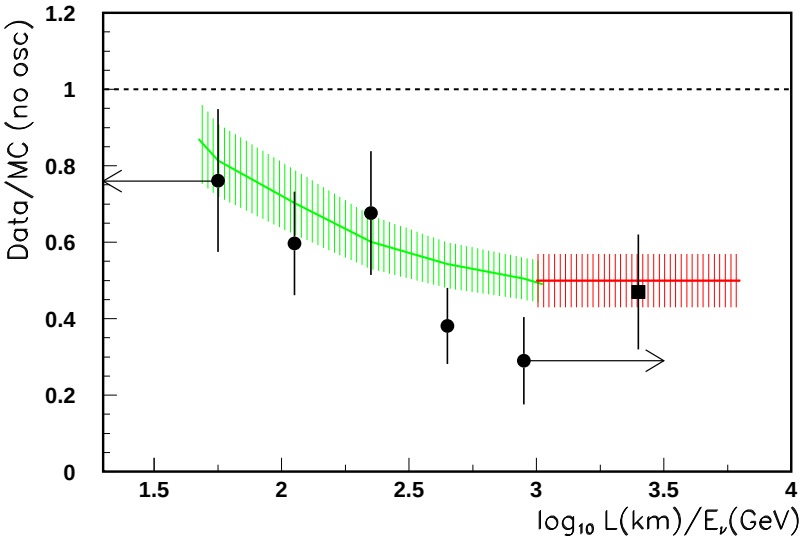

Figure 9: Ratio (Data/MC) as a function of estimated L/E_ν for the upthrougoing muon sample (black circles) and the semicontained up-μ (black square). For upthroughgoing muons the muon energy was estimated by MCS and E_ν by MC methods. The shaded regions represent the uncertainties in the MC predictions assuming $\sin^2 2\theta = 1$ and $\Delta m^2 = 0.0025$ eV^2. The horizontal dashed line at Data/MC=1 is the expectation for no oscillations.

distribution quite compatible with neutrino oscillations with the parameters of Section 3.1 [38].

As the interesting energy region for atmospheric neutrino oscillations spans from $\sim$ 1 GeV to some tens of GeV, it is important to improve the spatial resolution of the detector to push the saturation point as high as possible. For this purpose, a second analysis was performed with the streamer tubes in "drift mode", using the TDC's included in the QTP system, originally designed for the search for magnetic monopoles. To check the electronics and the feasibility of the analysis, two tests were performed at the CERN PS-T9 and SPS-X7 beams [64]. The space resolution achieved is $\simeq 3$ mm, a factor 3.5 better than in the first analysis. For each muon, seven MCS sensitive variables were given in input to a Neural Network (NN) previously trained to estimate the muon energy with MC events of known input energy crossing the detector at different zenith angles. The NN output allowed to separate the upthroughgoing muons in 4 subsamples with average energies of 12, 20, 50 and 102 GeV, respectively. The comparison of their zenith angle distributions with the predictions of the no oscillations MC shows a disagreement at low energies (where there is a deficit of vertical events), while the agreement is restored at increasing neutrino energies. The distribution of the ratio $R = (Data/MC_{noosc})$ obtained by this analysis is plotted in Fig. 9 as a function of $log_{10}(L/E_\nu)$ [50, 63, 69]. The black points with error bars are the data; the vertical extent of the shaded areas represents the uncertainties on the MC predictions for $\nu_\mu \rightarrow \nu_\tau$ oscillations with maximal mixing and $\Delta m^2 = 2.5 \cdot 10^{-3}$ eV^2. The horizontal dashed line is the expectation without oscillations. The last data point (black square) has been obtained from the low energy IU sample.

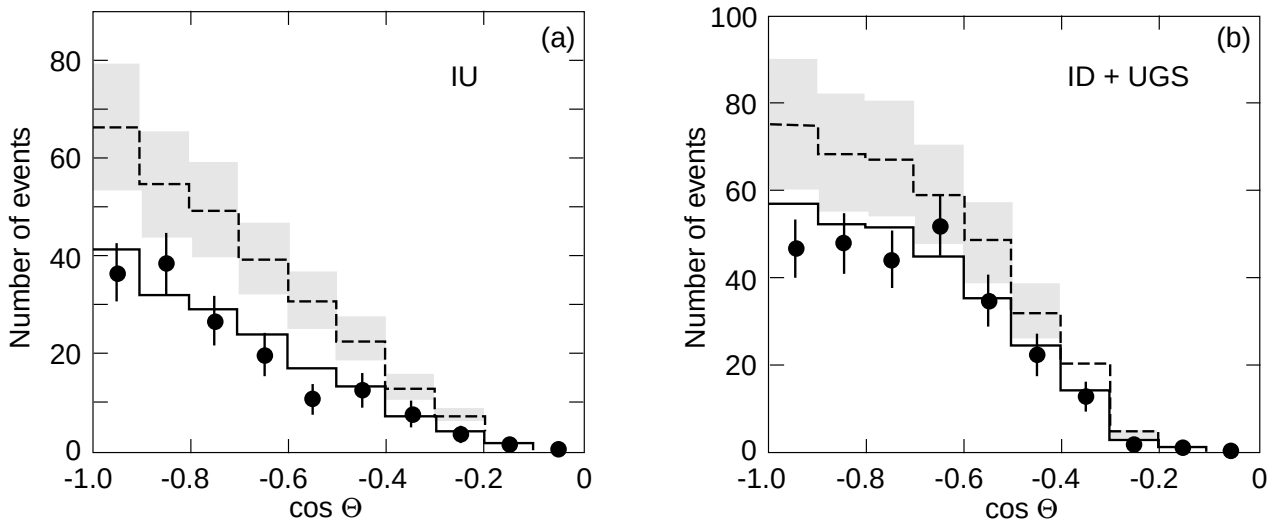

(a) (b)

Figure 10: Measured zenith distributions (a) for the upsemicontained (IU) events and (b) for the upstopping plus the downsemicontained (ID+UGD) events. The black points are the data, the dashed line at the center of the shaded regions correspond to MC predictions assuming no oscillations. The full line is the expectation for $\nu_\mu \to \nu_\tau$ oscillations with maximal mixing and $\Delta m^2 = 2.5 \cdot 10^{-3}\,\mathrm{eV}^2$.

3.4 Low energy data.

The *Internal Upgoing* (IU) muons come from ν_μ interactions in the lower apparatus [31]. Since two scintillation counters are intercepted, the T.o.F. is applied to identify the upward going muons (Fig. 2). The average parent neutrino energy for these events is 4.2 GeV (Fig. 5). If the atmospheric neutrino anomalies were the results of $\nu_\mu \to \nu_\tau$ oscillations with maximal mixing and Δm^2 between 10^{-3} and 10^{-2} eV^2, one would expect a reduction by about a factor of two in the flux of these events, without any distortion in the shape of the angular distribution. This is what is observed in Fig. 10a.

The *upstopping muons* (UGS) are due to external ν_μ interactions yielding upgoing muons stopping in the detector. The data correspond to an effective livetime of 5.6 y. The *semicontained downgoing muons* (ID) are due to ν_μ-induced downgoing tracks with vertex in the lower MACRO (Fig. 2). The two types of events are identified by means of topological criteria; the lack of time information prevents to distinguish the two sub-samples. An almost equal number of UGS and ID events is expected. In case of oscillations with the quoted parameters, the flux of the UGS should be reduced by 50%, the same amount of the ID muons at $cos\theta \simeq -1$. No reduction is instead expected for the semicontained downgoing events (coming from neutrinos having path lengths of ~ 20 km).

MC simulations for the low energy data use the Bartol neutrino flux and the neutrino low energy cross sections of ref. [72]. The number of events and the angular distributions are compared with MC predictions in Table 1 and Figs. 10a,b. The low energy data show

	Events	MC-No oscillations	$R = (Data/MC_{noosc})$
Up throughgoing	809	1122 ± 191	$(0.721 \pm 0.026_{stat} \pm 0.043_{sys} \pm 0.123_{th})$
Internal Up	154	$285 \pm 28_{sys} \pm 71_{th}$	$(0.54 \pm 0.04_{stat} \pm 0.05_{sys} \pm 0.13_{th})$
Up Stop + In Down	262	$375 \pm 37_{sys} \pm 94_{th}$	$(0.70 \pm 0.04_{stat} \pm 0.07_{sys} \pm 0.17_{th})$

Table 1: Summary of the MACRO $\nu_\mu \to \mu$ events in $-1 < cos\theta < 0$ after background subtraction. For each topology (see Fig. 2) the number of measured events, the MC prediction for no-oscillations and the ratio (Data/MC-no osc) are given.

a uniform deficit of the measured number of events for the whole angular distribution with respect to predictions, $\sim 50\%$ for IU, 75% for ID + UGS; there is good agreement with the predictions based on neutrino oscillations with the parameters obtained from the upthroughgoing muons.

The average value of the double ratio $R = (Data/MC)_{IU}/(Data/MC)_{ID+UGS}$ over the measured zenith angle range is $R \simeq 0.77 \pm 0.07$; the error includes statistical and theoretical uncertainties; $R = 1$ is expected in case of no oscillations [59].

4 Search for Astrophysical Point Sources of High Energy Muon Neutrinos

High energy ν_μ are expected to come from several galactic and extragalactic sources. Neutrino production requires astrophysical accelerators of charged particles and some kind of astrophysical beam dumps. The excellent angular resolution of our detector allowed a sensitive search for upgoing muons produced by neutrinos coming from celestial sources, with a negligible atmospheric neutrino background. An excess of events was searched for around the positions of known sources in 3° (half width) angular bins. This value was chosen so as to take into account the angular smearing produced by the multiple muon scattering in the rock below the detector and by the energy-integrated angular distribution of the scattered muon, with respect to the neutrino direction. Using a total livetime of 6.16 y (normalized to the complete configuration) we obtained a total of 1356 events, see Fig. 11. The 90% c.l. upper limits on the muon fluxes from specific celestial sources lay in the range $10^{-15} - 10^{-14}\,\mathrm{cm}^{-2}\,\mathrm{s}^{-1}$, see Fig. 11b (preliminary data were reported at the 2001 conferences) [37, 47, 56]. The solid MACRO line is our sensitivity vs. declination. Notice that we have two cases, GX339-4 ($\alpha = 255.71^o$, $\delta = -48.79^o$) and Cir X-1 ($\alpha = 230.17^o$, $\delta = -57.17^o$), with 7 events: in figure 11 they are considered as a background, therefore the upper flux limits are higher; but they could also be indication of signals.

We searched for time coincidences of our upgoing muons with γ-ray bursts as given in the BATSE 3B and 4B catalogues, for the period from April 91 to December 2000 [33]. No statistically significant time correlation was found.

We have also searched for a diffuse astrophysical neutrino flux for which we establish a flux upper limit at the level of $1.5 \cdot 10^{-14}\,\mathrm{cm}^{-2}\,\mathrm{s}^{-1}$ [56].

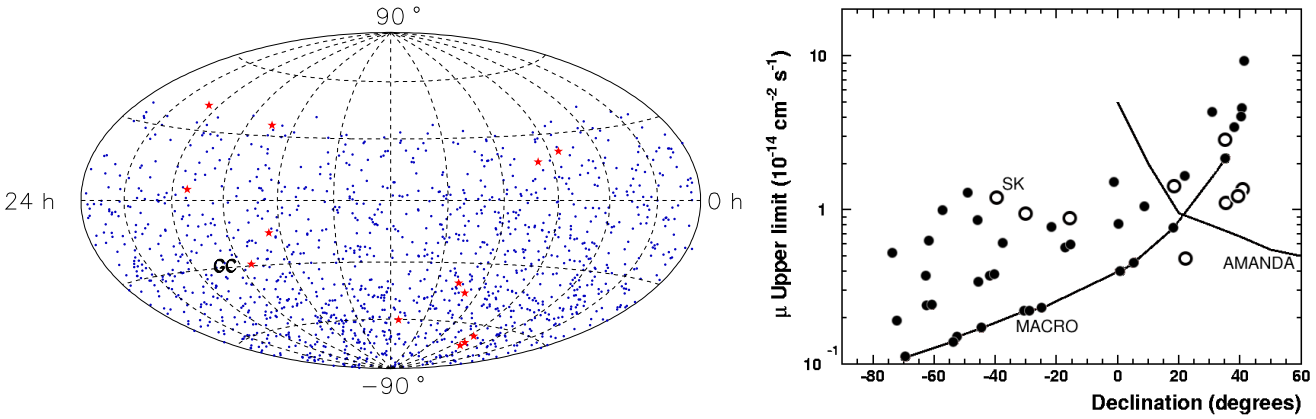

(a) (b)

Figure 11: High energy neutrino astronomy. (a) Upgoing muon distribution in equatorial coordinates (1356 events). (b) The black points are the MACRO 90 % c.l. upwardgoing muon flux limits as a function of the declination for 42 selected sources. The solid line refers to the MACRO limits obtained for those cases for which the atmospheric neutrino background was zero. The limits from the SK (open circles) and AMANDA (thin line) experiments are quoted; these last limits refer to much higher energy neutrinos.

5 Indirect Searches for WIMPs

Weakly Interacting Massive Particles (WIMPs) could be part of the galactic dark matter; WIMPs could be intercepted by celestial bodies, slowed down and trapped in their centers, where WIMPs and anti-WIMPs could annihilate and yield upthroughgoing muons. The annihilations in these celestial bodies would yield neutrinos of GeV or TeV energy, in small angular windows from their centers.

For the Earth we have chosen a 15^o cone around the vertical: we find 863 events. The MC expectation for atmospheric ν_μ without oscillations gives a larger number of events. We set a conservative flux upper limit assuming that the measured number of events equals the expected ones. We obtain the 90 % c.l. MACRO limits for the flux of upgoing muons as shown in Fig. 12a (it varies from about 0.8 to 0.5 $10^{-14}\,\mathrm{cm}^{-2}\,\mathrm{s}^{-1}$). If the WIMPs are identified with the smallest mass neutralino, the MACRO limit may be used to constrain the stable neutralino mass, following the model of Bottino et al. [73], see Figure 12a.

A similar procedure was used to search for muon neutrinos from the Sun, using 10 search cones from 3^o to 30^o. In the absence of statistically significant excesses the muon upper limits are at the level of about $1.5 - 2 \cdot 10^{-14}\,\mathrm{cm}^{-2}\,\mathrm{s}^{-1}$ are established. The limits are shown in Fig. 12b as a function of the WIMP (neutralino) mass.

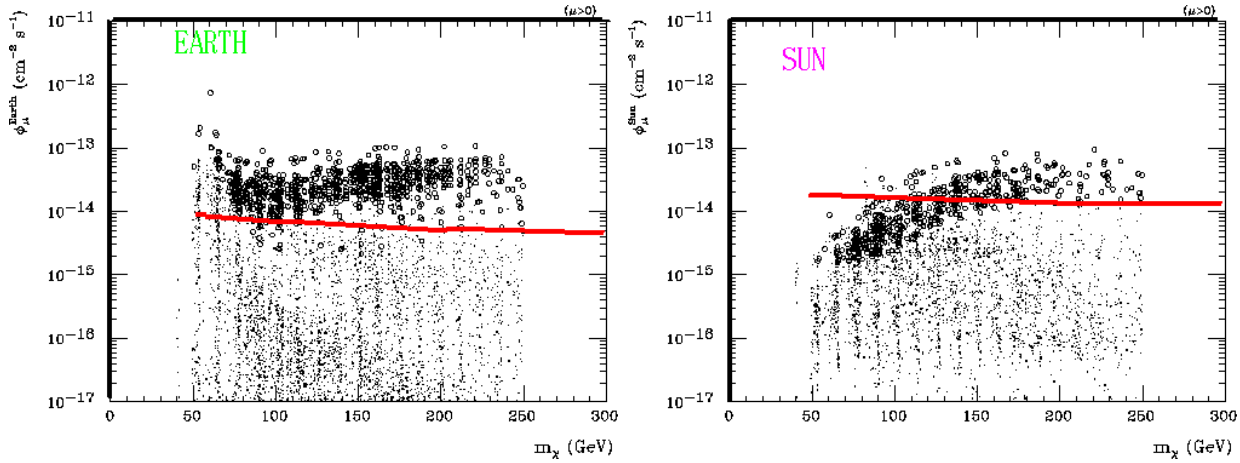

(a) (b)

Figure 12: (a) The solid line is the MACRO upwardgoing muon flux upper limit (90%c.l.) from the Earth plotted vs. neutralino mass m_χ for $E_\mu{}^{th} = 1\,\mathrm{GeV}$. (b) The same as in (a) but for upwardgoing muons from the Sun [28]. Each dot is obtained varying model parameters. The open circles indicate models *excluded* by direct measurements (in particular the DAMA/NaI experiment [74]) and assume a local dark matter density of about $0.5\,\mathrm{GeVcm}^{-3}$.

6 Magnetic Monopoles and Nuclearites

The search for magnetic monopoles (MM) was one of the main objectives of our experiment. Supermassive monopoles predicted by Grand Unified Theories (GUT) of the electroweak and strong interactions should have masses of the order of $m_M \sim 10^{17}\,\mathrm{GeV}$.

These monopoles could be present in the penetrating cosmic radiation and are expected to have typical galactic velocities, $\sim 10^{-3}c$, if trapped in our Galaxy. MMs trapped in our solar system or in the supercluster of galaxies may travel with typical velocities of the order of $\sim 10^{-4}c$ and $\sim 10^{-2}c$, respectively. Monopoles in the presence of strong magnetic fields may reach higher velocities. Possible intermediate mass monopoles could reach relativistic velocities.

The reference sensitivity level for a significant MM search is the Parker bound [75], the maximum monopole flux compatible with the survival of the galactic magnetic field. This limit is of the order of $\Phi \lesssim 10^{-15}\,\mathrm{cm}^{-2}\,\mathrm{s}^{-1}\,\mathrm{sr}^{-1}$, but it could be reduced by almost an order of magnitude when considering the survival of a small galactic magnetic field seed [75]. Our experiment was designed to reach a flux sensitivity well below the Parker bound, in the MM velocity range of $4 \times 10^{-5} < \beta < 1$. The three MACRO sub-detectors have sensitivities in wide β-ranges, with overlapping regions; thus they allow multiple signatures of the same rare event candidate. No candidates were found in several years of data taking by any of the three subdetectors.

The MM flux limits set by several different analyses using the three subdetectors over different β-range were combined to obtain a global MACRO limit. For each β value, the global time integrated acceptance was computed as the sum of the independent portions of each analysis. Our limits are shown in Fig. 13 versus β together with the limits set by

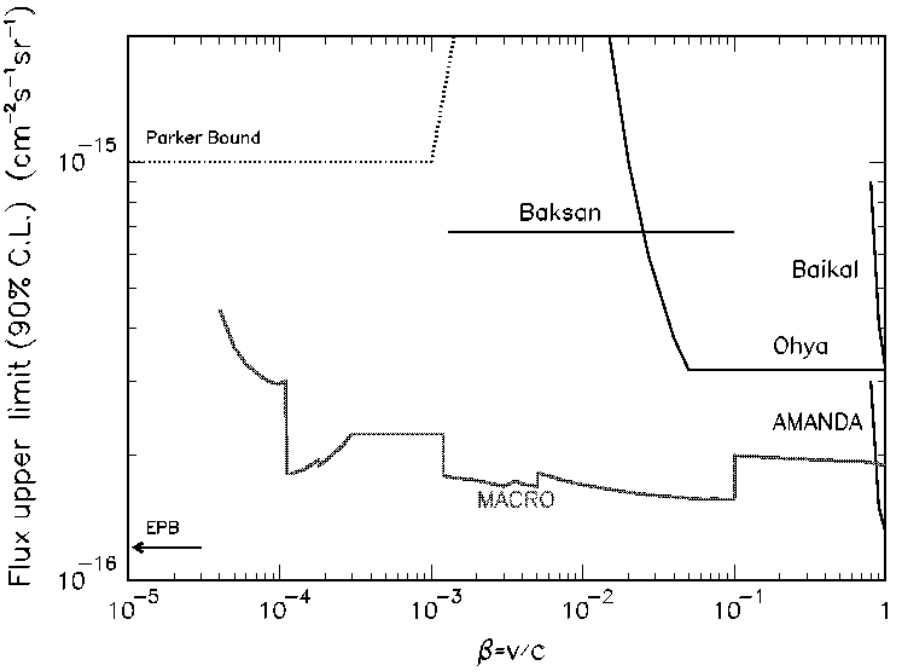

Figure 13: Magnetic monopole flux upper limits at the 90% c.l. obtained by MACRO and by other experiments [75, 77, 78]. The limits apply to singly charged ($g = g_D$) monopoles assuming that catalysis cross sections are smaller than a few mb.

other experiments [75, 77, 78]; other limits are quoted in [36, 43, 49, 62, 79]. Our MM limits are the best existing over a wide range of β , $4 \times 10^{-5} < \beta < 1$.

A specific search for monopole catalysis of nucleon decay was made with the streamer tube system [58]. Since no event was found, we can place a monopole flux upper limit at the level of $\sim 3 \cdot 10^{-16}\, cm^{-2} s^{-1} sr^{-1}$ for $10^{-4} \lesssim \beta \lesssim 5 \cdot 10^{-3}$, valid for a large catalysis cross section, $5 \cdot 10^2 < \sigma_{cat} < 10^3\, mb$. The flux limit for the standard direct MM search with streamer tubes is valid for $\sigma_{cat} < 100\, mb$.

The MM searches based on the scintillator and on the nuclear track subdetectors were also used to set new upper limits on the flux of cosmic ray nuclearites (strange quark matter), over the same β range, Fig. 14. If nuclearites are part of the dark matter in our galaxy, the most interesting β is of the order of $\sim 10^{-3}$. Fig. 14 shows our limit plotted vs nuclearite mass for $\beta = 2 \times 10^{-3}$ (at ground level). Other experimental limits are also shown.

Some of the nuclearite limits apply also to Q-balls (agglomerates of squarks, sleptons and Higgs fields) [58, 62].

The energy losses of MMs, dyons and of other heavy particles in the Earth and in different detectors for various particle masses and velocities were computed in [76].

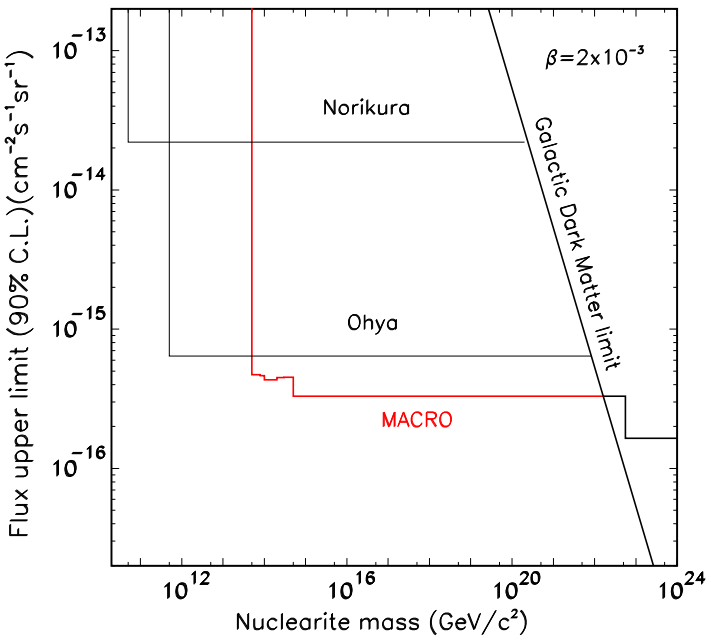

Figure 14: 90% c.l. flux upper limits vs. mass for nuclearites with $\beta = 2 \cdot 10^{-3}$ at ground level. Nuclearites of such velocity could have galactic or extragalactic origin. The MACRO direct limit (solid line) is shown along with the other direct limits [77, 78]; the indirect mica limits of [80, 81] are at the level of $2 \cdot 10^{-20} cm^{-2} s^{-1} sr^{-1}$. The limits for nuclearite masses larger than $5 \cdot 10^{22}$ GeVc^{-2} correspond to an isotropic flux.

7 Neutrinos from Stellar Gravitational Collapses

A stellar gravitational collapse (GC) of the core of a massive star is expected to produce a large burst of all types of neutrinos and antineutrinos with energies of $7 - 30$ MeV and with a duration of ~ 10 s. The $\bar{\nu}_e$'s can be detected via the process $\bar{\nu}_e + p \rightarrow n + e^+$ in the liquid scintillator. About $100 \div 150$ $\bar{\nu}_e$ events should be detected in our 580 t scintillator for a stellar collapse at the center of our Galaxy.

We used two electronic systems for detecting $\bar{\nu}_e$'s from stellar gravitational collapses. The first system was based on the dedicated PHRASE trigger, the second one was based on the ERP trigger. Both systems had an energy threshold of ~ 7 MeV and recorded pulse shape, charge and timing informations. Immediately after a > 7 MeV trigger, the PHRASE system lowered its threshold to about 1 MeV, for a duration of 800μs, in order to detect (with a $\simeq 25\,\%$ efficiency) the 2.2 MeV γ released in the reaction $n + p \rightarrow d + \gamma_{2.2\,\mathrm{MeV}}$ induced by the neutron produced in the primary process.

A redundant supernova alarm system was in operation, alerting immediately the physicists on shift. We defined a general procedure to alert the physics and astrophysics communities in case of an interesting alarm. Finally, a procedure to link the various supernova observatories around the world was set up [23].

The effective MACRO active mass was ~ 580 t; the live-time fraction in the last four years was $\simeq 97.5\,\%$. No stellar gravitational collapses were observed in our Galaxy from the beginning of 1989 to the end of 2000 [42].

8 Cosmic Ray Muons

The large area and acceptance of our detector allowed the study of many aspects of physics and astrophysics of cosmic rays (CR). We recorded $\sim 6 \times 10^7$ single muons and $\sim 3.7 \times 10^6$ multiple muons at the rate of $\sim 18,000$/day.

Muon vertical intensity. The underground muon vertical intensity vs. rock thickness provides information on the high energy ($E \gtrsim 1.3\,\mathrm{TeV}$) atmospheric muon flux and on the all-particle primary CR spectrum. The results can be used to constrain the models of cosmic ray production and interaction. The analysis performed in 1995 covered the overburden range $2200 \div 7000\,\mathrm{hg/\,cm^2}$ [16].

Analysis of high multiplicity muon bundles. The study of the **multiplicity distribution** of muon bundles provides informations on the primary CR composition model. The study of the **decoherence** function (the distribution of the distance between two muons in a muon bundle) provides informations on the hadronic interaction features at high energies; this study was performed using a large sample of data and improved Monte Carlo methods, see Fig. 15a [29]. We used different hadronic interaction models (DPMJET, QGSJET, SIBYLL, HEMAS, HDPM) interfaced to the HEMAS and CORSIKA shower propagation codes [82].

We studied *muon correlations inside a bundle* [82], using the so called correlation integral [83], to search for correlations of dynamical origin in the bundles. Since the cascade development in atmosphere is mainly determined by the number of "steps" in the "tree formation", we expect a different behaviour for cascades originated by light and heavy CR primaries. For the same reason, the analysis should be less sensitive to the hadronic interaction model adopted in the simulations. This analysis shows that, in the energy region above 1000 TeV, the composition model derived from the analysis of the muon multiplicity distribution [19, 20] is almost independent from the interaction model.

We also searched for *substructures ("clusters") inside muon bundles* [84]. The search for clusters was performed by means of different software algorithms; the study is sensitive both to the hadronic interaction model and to the primary CR composition model. If the primary composition has been determined by the first method, a choice of the bundle topology gives interesting connections with the early hadronic interaction features in the atmosphere. The comparison between our data and Monte Carlo simulations allowed to place constraints on the used interaction models. The same Monte Carlo study has shown that muon bundles with a central core and an isolated cluster with at least two muons are the result of random associations of peripheral muons. A combined analysis with the study of the decoherence function for high multiplicity events has shown that the hadronic interaction model that better reproduces the underground observables is QGSJET.

The ratio double muons/single muons: The ratio N_2/N_1 of double muon events over single muon events is expected to decrease at increasing rock depths, unless some exotic phenomena occur. The ratio N_2/N_1 was studied in underground experiments and in phenomenological papers [85, 86]. The LVD collaboration reports that the ratio of multiple-muons to all-muons increases for rock depths $h > 7000\ hg/cm^2$.

We measured [57] the ratio N_2/N_1 as a function of the rock depth, using also multiple

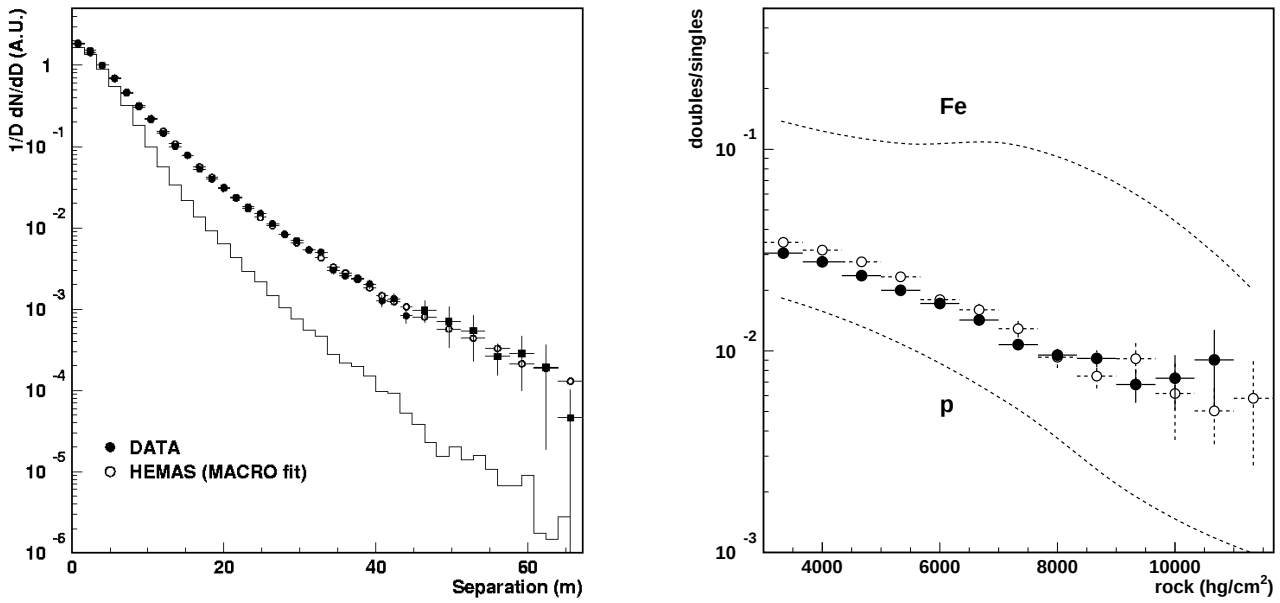

(a) (b)

Figure 15: (a) True unfolded experimental decoherence distribution for an infinite detector (black points) compared with MC expectations (open points); the measured decoherence distribution before unfolding is shown as an histogram [29]. (b) Ratio of double muon events to single muon events as a function of the rock depth. The black points are our data; the open circles are Monte Carlo predictions made using the MACRO composition model. Monte Carlo predictions using pure proton and iron primaries are shown as dashed lines.

muon events at large zenith angles. A detailed Monte Carlo simulation was made using the HEMAS code, where the event zenith angle can be extended up to 89°. The event direction is reconstructed by the tracking system. The rock depth is provided by the Gran Sasso map function $h(\theta, \phi)$, which extends up to $\theta = 94°$. The "true" muon multiplicity is the largest value among N_{HW} and N_{VW}, the multiplicities in the horizontal and vertical planes, respectively. Monte Carlo simulations have shown that the percentage of events with mis-reconstructed multiplicity is less that 3%. Attention was devoted to the "cleaning" of the events from spurious effects (electronic noise, radioactive background, etc); in many cases, we made a visual scanning of the events. Our measured ratios N_2/N_1 as a function of the rock depth, Fig. 15, are in agreement with the expectation of a monotonic decrease of N_2/N_1 down to $h \sim 10000\ hg/cm^2$. Above this value, the low statistics does not allow to state a firm conclusion on a possible increase of N_2/N_1.

Muon Astronomy. In the past, some experiments reported excesses of modulated muons from the direction of known astrophysical sources, f.e. Cyg X-3. Our data do not indicate significant excesses above background, both for steady dc fluxes and for modulated ac fluxes. The MACRO pointing precision was checked via the shadow of the Moon and of the Sun on primary cosmic rays. The pointing resolution was checked with double muons,

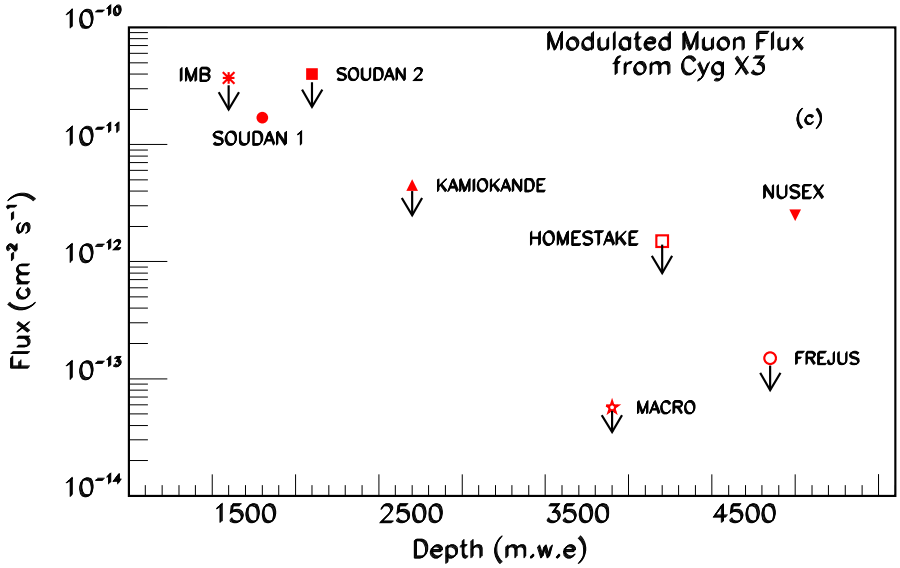

Figure 16: Present situation of the searches for a modulated muon signal from Cyg X-3. The Soudan 1 and Nusex collaborations reported positive indications, while all other experiments give flux upper limits.

assuming that they are parallel. The angle containing 68% of the events in a $\Delta\theta$ bin is 0.8^o, which we take as our resolution.

All sky d.c. survey. The sky, in galactic coordinates, was divided into bins of equal solid angle, $\Delta\Omega = 2.1 \cdot 10^{-3} sr$, $\Delta\alpha = 3^o$, $\Delta sin\delta = 0.04$; they correspond to cones of 1.5^o half angles. In order to remove edge effects, three other surveys were done, by shifting the map by one-half-bin in α (map 2), by one-half bin in sinδ (map 3) and with both α and sinδ shifted (map 4). For each solid angle bin we computed the deviation from the average measured muon intensity, after background subtraction, in units of standard deviations

$$\sigma(i) = \frac{N_{obs}(i) - N_{exp}(i)}{\sqrt{N_{exp}(i)}} \tag{1}$$

where $N_{obs}(i)$ is the observed number of events in bin i and N_{exp} is the number of events expected in that bin from the simulation. No deviation was found and for the majority of the bins we obtain flux upper limits at the level of ${\Phi_\mu}^{steady}(95\%) \leq 5 \times 10^{-13} cm^{-2} s^{-1}$.

Specific point-like d.c. sources. For Cyg X-3, Mrk421, Mrk501 we searched in a narrower cone (1^o half angle) around the source direction. We obtain flux limits at the level of $(2-4) \cdot 10^{-13} cm^{-2} s^{-1}$. There is a small excess of 2.0 σ in the direction of Mrk501.

Modulated a.c. search from Cyg X-3 and Her X-1. No evidence for an excess was observed and the limits are $\Phi < 2 \times 10^{-13} cm^{-2} s^{-1}$; see Fig. 16 .

Search for bursting episodes. We made a search for pulsed muon signals in a 1^o half angle cone around the location of possible sources of high energy photons. Bursting episodes

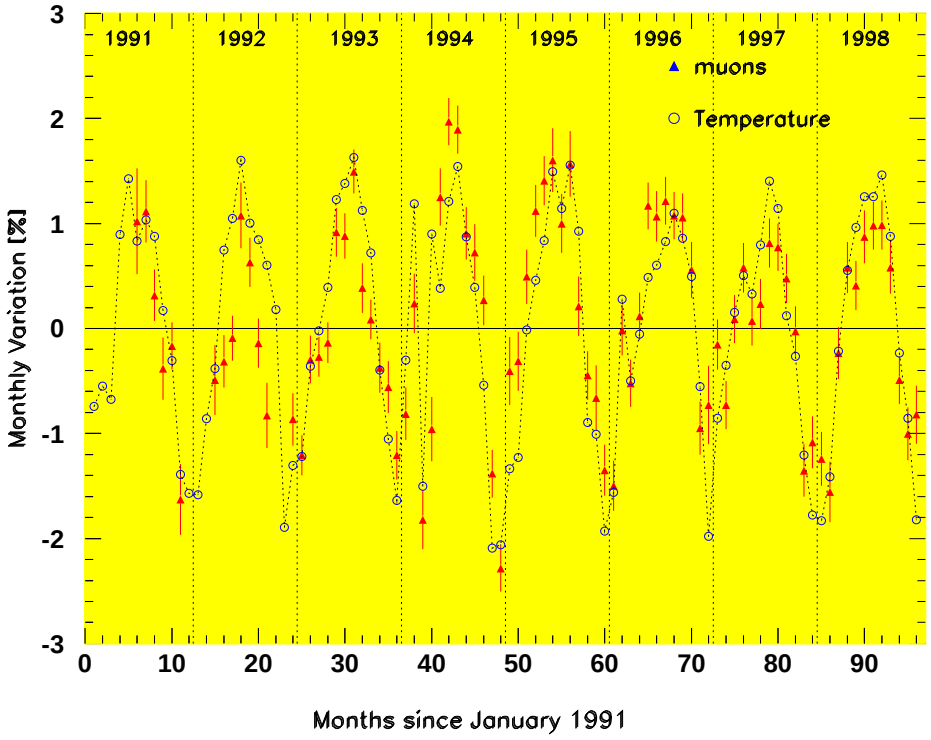

Figure 17: Seasonal variation of the muon flux from above (black triangles); the open circles are measurements of the temperature of the upper atmosphere.

of duration of ~ 1 day were searched for with two different methods. In the first method we searched for daily excesses of muons above the background, also plotting cumulative excesses day by day. In the second method we computed day by day the quantity $-Log_{10}P$ where P is the probability to observe a burst at least as large as N_{obs}. We find some possible excesses for Mrk421 on the days 7/1/93, 14/2/95, 27/8/97, 5/12/98.

Seasonal variations. Underground muons are produced by mesons decaying in flight in the atmosphere. The muon flux thus depends on the ratio between the decay and the interaction probability of the parent mesons, which are sensitive to the atmospheric density and to the average temperature. The flux is expected to decrease in winter, when the temperature is lower and the atmosphere more dense, and to increase in summer. We find the expected variations at the level of $\pm 2\%$ [21], see Fig. 17.

Solar daily variations. Because of variations in the day-night temperatures we expect solar daily variations similar to seasonal variations, but of considerably smaller amplitudes. Using the total MACRO data, we find these variations with an amplitude $A = (0.88 \pm 0.26) \cdot 10^{-3}$ with a significance of about 3.4 σ, see Fig. 18a.

Sidereal anisotropies are due to the motion of the solar system through the "sea" of relativistic cosmic rays in our galaxy. They are expected to yield a small effect. After a correction due to the motion of the Earth around the Sun, we observe variations with an

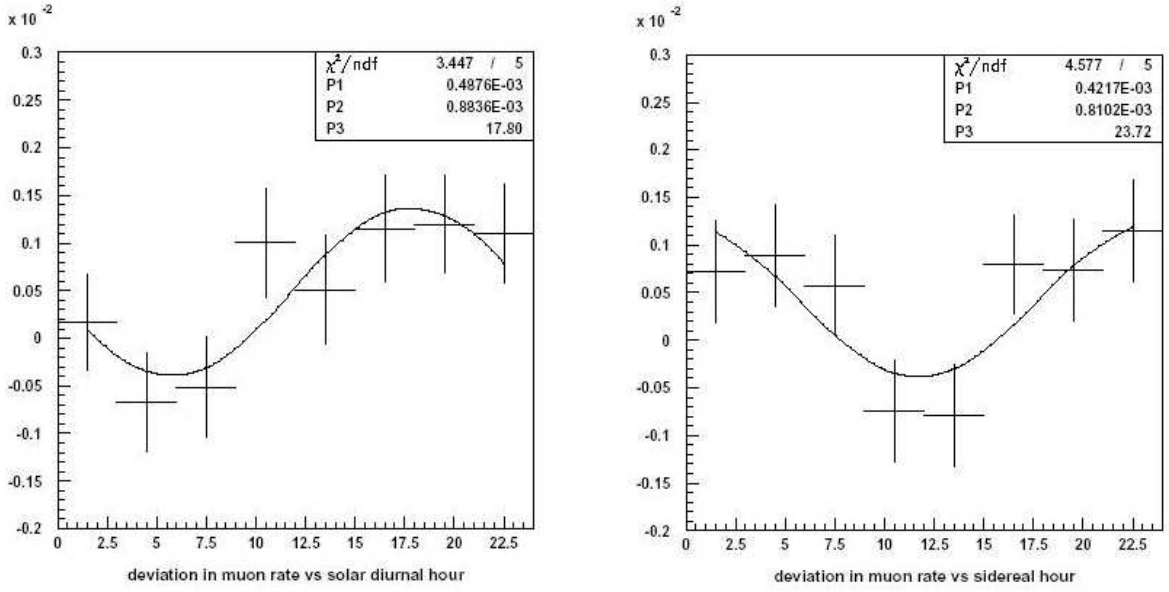

(a) (b)

Figure 18: Deviations of the muon rate from the mean muon rate (a) versus the local solar diurnal time at Gran Sasso, and (b) versus the local sidereal time.

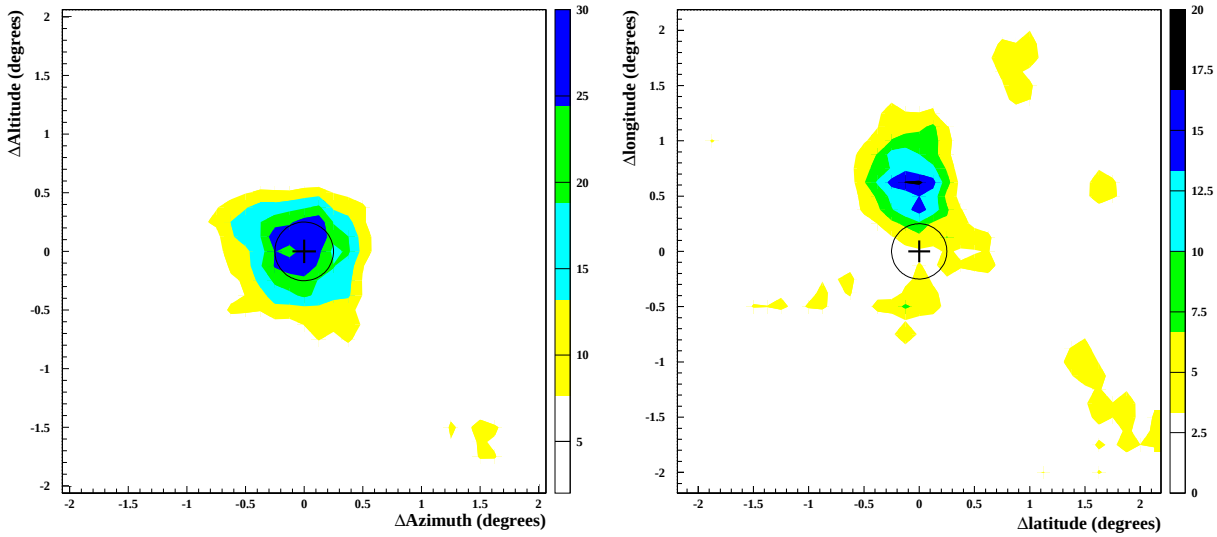

(a) (b)

Figure 19: Moon and sun shadows. (a) Two dimensional distributions of the muon event density around the moon direction. The various regions of increasing gray scale indicate various levels of deficit in percent. The darkest one corresponds to the maximum deficit. (b) Same analysis for the sun direction.

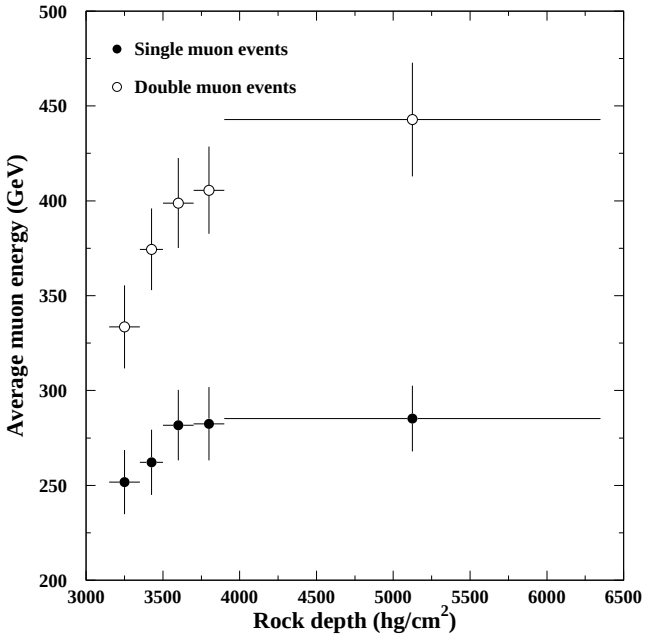

Figure 20: Residual average muon energy at the underground Gran Sasso lab versus standard rock depth for single muons and for double muons [27], see text.

amplitude of $8.6 \cdot 10^{-4}$ and a phase $\phi_{max} = 22.7^{\circ}$ with a statistical significance of 3 σ, Fig. 18b.

Moon and sun Shadows of primary cosmic rays. The pointing capability of MACRO was demonstrated by the observed "shadows" of the Moon and of the Sun, which produce a "shield" to the cosmic rays. We used a sample of $45 \cdot 10^6$ muons, looking at the bidimensional density of the events around the directions of the Moon and of the Sun [26][53]. In Fig. 19 we show two-dimensional plots of the muon deficits caused by the Moon and the Sun. For the Moon: we looked for events in a window $4.375^o \times 4.375^o$ centered on the Moon; the window was divided into 35×35 cells, each having dimensions of $0.125^o \times 0.125^o$ ($\Delta\Omega = 1.6 \cdot 10^{-2} deg^2$). In the bidimensional plot of Fig. 19a one observes a depletion of events with a statistical significance of 5.5 σ. The observed slight displacement of the maximum deficit is consistent with the displacement of the primary protons due to the geomagnetic field. We repeated the same analysis for muons in the sun window, Fig. 19b. The difference between the apparent sun position and the observed muon density is due to the combined effect of the magnetic field of the Sun and of the Earth. The observed depletion has a statistical significance of 4.5 σ.

9 Muon energy measurement with the TRD detector

The underground differential energy spectrum of muons was measured with the three TRD modules detector. We analyzed two types of events: "single muons", i.e. single

events in MACRO crossing a TRD module, and "double muons", i.e. double events in MACRO with only one muon crossing the TRD detector.The measurements refer to muons with energies $0.1 < E_\mu < 1\,\mathrm{TeV}$ and for $E_\mu > 1\,\mathrm{TeV}$ [27]. In order to evaluate the local muon energy spectrum, we must take into account the TRD response function, which induces some distortion of the "true" muon spectrum distribution. The "true" distribution was extracted from the measured one by an unfolding procedure that yields good results only if the response of the detector is correctly understood. We used an unfolding technique developed according to Bayes' theorem. Fig. 20 shows the average muon energies versus standard rock thickness for single and double muons. Systematic uncertainties are included in the error bars. The average single muon energy at the Gran Sasso underground lab is 270 GeV; for double muons it is ~ 380 GeV. Double muons are more energetic than single muons; this is in agreement with the predictions of interaction models of primary CRs in the atmosphere.

10 EAS-TOP/MACRO Coincidence Experiment

For coincident events, EASTOP measured the e.m. size of the showers above the surface (at Campo Imperatore), while MACRO measured penetrating muons underground. The purpose is to study the primary cosmic ray composition versus energy reducing the dependence on the interaction and propagation models. The two completed detectors operated in coincidence for a livetime of 960.1 days. The number of coincident events is 28160, of which 3752 have shower cores inside the edges of the EASTOP array ("internal events") and shower sizes $N_e > 2 \cdot 10^5$; 409 events have $N_e > 10^{5.92}$, i.e. above the CR knee. The data have been analyzed in terms of the QGSJET interaction model as implemented in CORSIKA [90].

The e.m. detector of EASTOP is made of 35 scintillator modules, 10 m^2 each, covering an area of $\simeq 10^5\,\mathrm{m}^2$. The array is fully efficient for $N_e > 10^5$. The reconstruction capabilities of the extensive air shower (EAS) parameters for internal events are: $\frac{\Delta N_e}{N_e} \simeq 10\%$ for $N_e \gtrsim 10^5$, and $\Delta\theta \sim 0.9^o$ for the EAS arrival direction [91].

We considered in MACRO muon tracks with at least 4 aligned hits in both views of the horizontal streamer tube planes. The muon energy threshold at the surface inside the effective area of EAS-TOP, for muons reaching the MACRO depth, ranges from 1.3 TeV to 1.8 TeV. Event coincidence is made off-line, using the absolute time given by a GPS system with an accuracy of better than 1 μs. Independent analyses of the MACRO and of the EAS-TOP data are described in [20] and [92], respectively.

The main experimental features considered are the muon multiplicity distributions in six different intervals of shower sizes. For each size bin the muon multiplicity distribution was fitted with a superposition of (i) pure p and Fe components, or (ii) light (L) and heavy (H) admixtures containing equal fractions of p and He or Mg and Fe, respectively. All spectra in the simulation have slope $\gamma = 2.62$. In each of the six windows we minimized

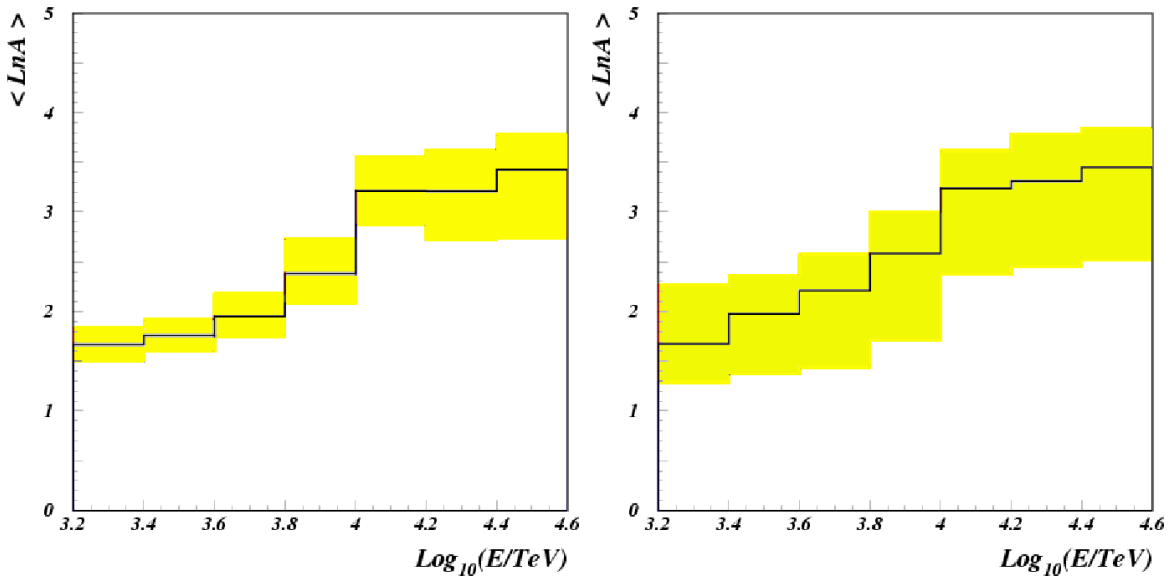

Figure 21: EASTOP-MACRO coincidences. $\langle lnA \rangle$ vs primary energy for: (a) p/Fe and (b) $Light/Heavy$ compositions. The histograms (black lines) are obtained from the data, the shaded areas include the uncertainties discussed in the text.

$$\chi^2 = \sum_i \frac{(N_i^{exp} - p_1 N_i^p - p_2 N_i^{Fe})^2}{\sigma_{i,exp}^2} \tag{2}$$

where N_i^{exp} is the number of observed events in the i-th bin, N^p (N^L) and N^{Fe} (N^H) are the number of simulated events in the same bin, p_1 and p_2 are the parameters (to be fitted) defining the fraction of each mass component in the same multiplicity bin.

For each size bin we take from the simulation the $log_{10}(E)$ distributions of contributing mass groups weighted by the parameters p_1 and p_2 with weights w_k representing the relative efficiency to trigger the underground apparatus. The resulting distributions from different size bins are summed together, and we obtain the simulated energy spectra of the two basic components that reproduce the experimental data. The values of the fitting parameters p_1 and p_2 have been used to compute the average $\langle lnA \rangle$; Fig. 21 shows $\langle lnA \rangle$ versus $log_{10}E$ (E in TeV); the shaded regions include the uncertainties in the fitting parameters p_1 and p_2 for (a) the p/Fe composition model and (b) for the light/heavy model.

Fig. 21 shows the results of the fits, plotted as $\langle lnA \rangle$ versus $log_{10}E$ (E in TeV); the shaded regions include the uncertainties in the fitting parameters p_1 and p_2 for (a) the p/Fe composition model and (b) for the light/heavy model. The results show an increase of $\langle lnA \rangle$ with energy in the CR knee region. The results are in agreement with the measurements of EAS-TOP alone at the surface using the same (QGSJET) interaction model.

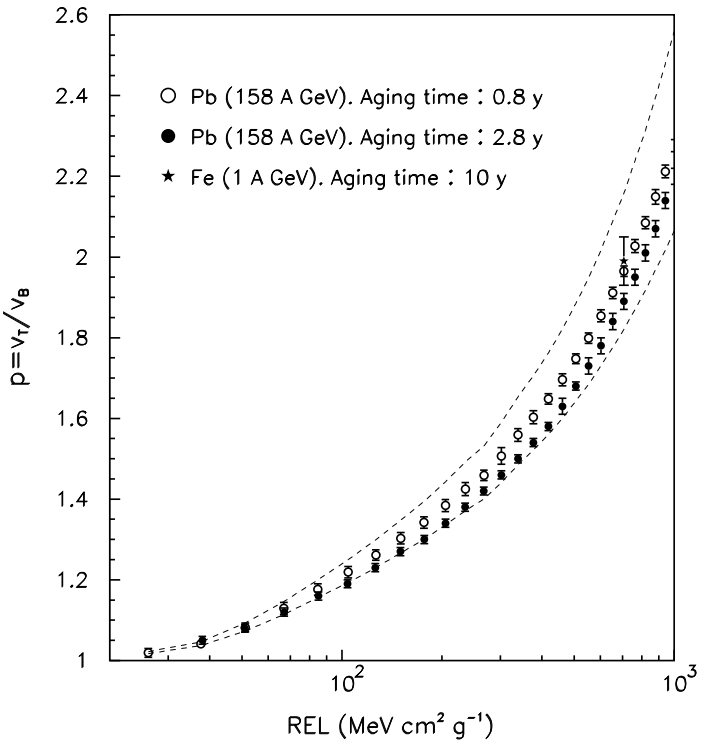

Figure 22: $p = v_T/v_B$ vs. REL for CR39 exposed to $^{2}07Pb^{8}2+$ ions of 158 A GeV and $^{5}6Fe^{2}6+$ ions of 1A GeV at different times after production. This was done to estimate possible aging effects. The dashed lines indicate the systematic uncertainty arising mainly from fluctuations of the bulk etching rate v_B.

Our data also agree with the results of the Kascade experiment. The EAS-TOP and MACRO coincidences offered the unique opportunity of measuring the lateral distribution of Cherenkov light in the $10 \div 100$ TeV energy range by associating the Cherenkov light collected by the EAS-TOP telescopes with the TeV muon through MACRO. We compared the measured Cherenkov light lateral distribution with simulations based on the CORSIKA-QGSJET code used for the composition analysis; this check provided an experimental validation of the code [90].

11 Nuclear Track Detector Calibrations

We performed further calibrations of the nuclear track detector CR39 with both slow and fast ions. In all measurements we have seen no deviation of its response from the Restricted Energy Loss (REL) model. To complete the calibration, nuclear track detector stacks of CR39 and Lexan foils, placed before and after various targets, were exposed to 158 A GeV Pb^{82+} ions at the CERN-SPS and to 1 A GeV Fe^{26+} ions at the BNL-AGS. In traversing the target, the beam ions produce nuclear fragments with $Z < 82e$ and $Z < 26e$ for the lead and iron beams, respectively; this allows a measurement of the response of the detector in a Z region relevant to the detection of magnetic monopoles.

Previous analyses have shown that the CR39 charge resolution is about $0.19e$ in the range $72e \leq Z \leq 83e$ (obtained by measurements of the etch-cone heights); at lower Z the measurement of the cone base diameters allow to separate the different charges. Tests were made looking for a possible dependence of the CR39 response from its age, i.e. from the time elapsed between the date of production and the date of exposure ("aging effect" [93]). Two sets of sheets, 0.8 y and 2.5 y old, were exposed in 1994 to 158 A GeV Pb^{82+} ions. For each detected nuclear fragment the reduced etch rate $p = v_T/v_B$ (v_T and v_B are the track and bulk etching rates, respectively) was computed and plotted in Fig. 22 vs REL. The dashed lines represent the systematic uncertainties coming mainly from the uncertainty on v_B. A recent test was made by exposing 10 years old CR39 samples to 1 A GeV Fe^{26+} ions; the detector response is shown as a black star in Fig. 22. Thus within experimental uncertainties, aging effects in the MACRO CR39 are negligible. Until now we etched 821 m^2 of CR39 detectors, of which 626 m^2 have been completely analyzed. As no candidates were found, the CR39 90% c.l. limit for an isotropic flux of monopoles with $\beta > 0.1$ is at the level of $2 \cdot 10^{-16}\ cm^{-2}s^{-1}sr^{-1}$.

12 Search for Lightly Ionizing Particles

Fractionally charged particles could be expected in Grand Unified Theories as deconfined quarks; the expected charges range from Q=$e/5$ to Q=e 2/3. They should release a fraction $(Q/e)^2$ of the energy deposited by a muon traversing a medium. Lightly Ionizing Particles (LIPs) have been searched for in MACRO using a four-fold coincidence between three layers of scintillators and the streamer tube system [32]. The 90 % c.l. flux upper limits for LIPs with charges $2e/3$, $e/3$ and $e/5$ are presently at the level of $1.5 \cdot 10^{-15} cm^{-2}s^{-1}sr^{-1}$.

13 Conclusions

The MACRO detector took data from 1989 to the end of year 2000. In 2001 we have extended most of our analyses and searches. We would like to stress that MACRO obtained important results in all the items listed in the proposal :

- GUT Magnetic Monopoles. We now have the best flux upper limit over the widest β range, thanks to the large acceptance and the redundancy of the different techniques employed. This limit value is a unique result and it will stand for a long time.

- Atmospheric neutrino oscillations. In this field MACRO has had its major achievements. Analyses of different event topologies, different energies, the exploitation of Coulomb multiple scattering in the detector give strong support to the hypothesis of $\nu_\mu \rightarrow \nu_\tau$ oscillations.

- High energy muon neutrino astronomy. MACRO has been highly competitive with other underground experiments thanks to its good angular accuracy. It has been

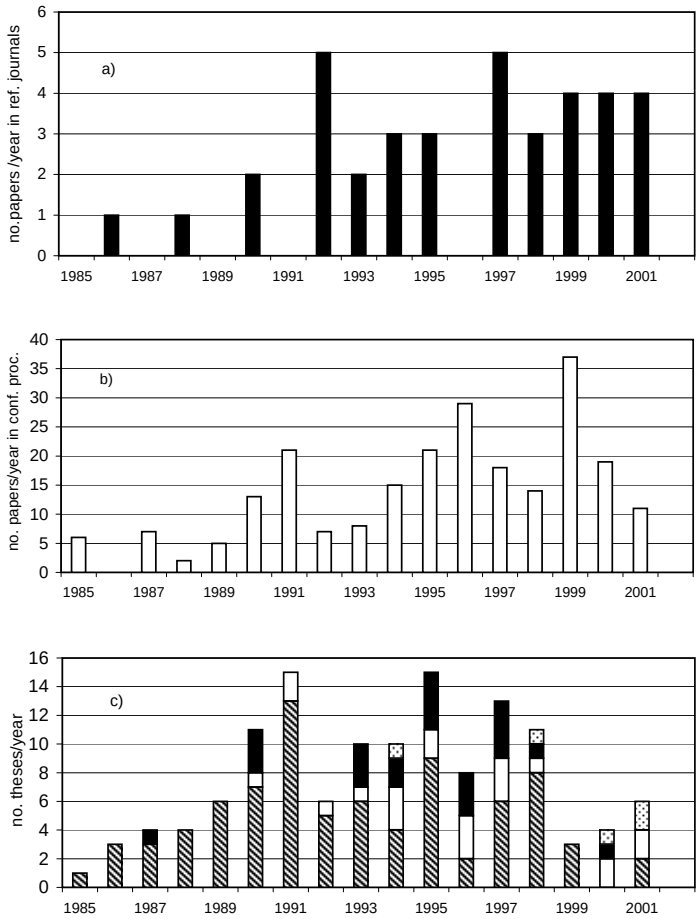

Figure 23: Time evolution of the MACRO publications: (a) in refereed journals, (b) in proceedings of conferences, (c) MACRO theses (the dashed boxes indicate Laurea theses, black boxes American PhD theses, white boxes Italian PhD theses, points theses de Doctorat Nationales).

limited only by its livetime and the size of the detector.

- Search for bursts of $\bar{\nu}_e$ from stellar gravitational collapses. In this field MACRO was sensitive to supernova events in the Galaxy, it started the SN WATCH system, and for a certain time it was the only detector in operation.

- Cosmic ray downgoing muons. MACRO observed the shadows of primary cosmic rays by the Moon and the Sun; this is also a proof of our pointing capability. We observed the seasonal variation ($\sim 2\%$ amplitude) over many years. We observed solar and sidereal variations with reasonable statistical significances even if the amplitudes of the variations are small (0.08%). No excesses of secondary muons attributable to astrophysical point sources (steady, modulated or bursting) were observed. The limits obtained are the best of any underground detector.
  We used multi-parameter fits and improved Monte Carlo simulations to explore the CR composition around the "knee" of the primary CR energy spectrum.

- Results have been obtained by studying the coincidence events between MACRO and the EASTOP array. This item represents a unique occasion as no other two experiments in such configuration exist. The number of events is limited due to the small common acceptance and short combined livetime. The data indicate an increase with increasing energy of the average Z of the primary CR nuclei.

- Sensitive searches for exotic particles have been carried out for possible Dark Matter candidates : (i) WIMPs, looking for upgoing muons from the center of the Earth and of the Sun; (ii) Nuclearites and Q-balls (obtained as byproducts of MM searches). (iii) Other limits concern possible Lightly Ionizing Particles.

Several of the above results (in particular the multiple Coulomb scattering analysis, the low energy neutrino data, etc) would have reached a greater significance if MACRO could have been granted an extension in data taking.

The dismantling of MACRO went regularly and essentially on schedule. We recuperated part of the electronics (modules, circuits, cables, etc) to be used in our Institutions, and donated the photomultipliers and part of the streamer tubes to other experiments.

The MACRO scientific and technical results have been

- published in 36 papers in refereed journals (we expect to publish 10 more with final results)

- published in 226 contributions to conferences and in invited papers

- discussed in about 534 Internal Memos

- used for 83 italian Laurea theses

- used for 22 italian Dottorato theses

- used for 23 US PhD theses

- used for 5 moroccan theses of Doctorat Nationales

Fig. 23 shows the time evolution of the published papers, conference proceedings and of the theses (Laurea, Dottorato, PhD, Doctorat Nationale).

Acknowledgments

We acknowledge the support of the Directors and of the staff of the Gran Sasso Laboratory and of the Institutions partecipating in the experiment. We thank the Istituto Nazionale di Fisica Nucleare (INFN), the US Department of Energy and the US National Science Foundation for their support. We acknowledge the strong cooperation of our technical staff, in particular of R. Assiro, E. Barbarito, A. Boiano, E. Bottazzi, P. Calligola, A. Candela, A. Ceres, D. Cosson, P. Creti, L. Degli Esposti, U. Denni, D. Di Ferdinando, R. Diotallevi, R. Farano, E. Favero, A. Frani, M. Gebhard, R. Giuliani, M. Goretti, H. Gran, A. Hawthorne, A. Leone, D. Margherita, V. Marrelli, F. Massera, S. Mengucci, M. Mongelli, L. Mossbarger, M.Orsini, S. Parlati, G.

Pellizzoni, M. Perchiazzi, C. Pinto, A. Sacchetti, P. Saggese, S. Sondergaards, S. Stalio, M. Vakili, C. Valieri and N. Zaccheo. We thank INFN-FAI, ICTP (Trieste), NATO and WorldLab for providing fellowships and grants for non-Italian citizens.

References

[1] MACRO Collaboration, C. De Marzo et al., "MACRO: a large area detector at the Gran Sasso laboratory", Nuovo Cimento 9C(1986)281.

[2] MACRO Collaboration, M.Calicchio et al., "The MACRO detector at the Gran Sasso laboratory", Nucl. Instr. Methods Phys. Res. A264(1988)18.

[3] MACRO-EASTOP Collaborations, R.Bellotti et al., M.Aglietta et al., "Simultaneous observation of the extensive air showers and deep underground muons at the Gran Sasso laboratory", Phys. Rev. D42(1990)1396.

[4] MACRO Collaboration, S.Ahlen et al., "Study of penetrating cosmic ray muons and search for large scale anisotropy at the Gran Sasso laboratory", Phys. Lett. B249(1990)149.

[5] MACRO Collaboration, S.Ahlen et al., "Arrival time distributions of very high energy cosmic ray muons in MACRO", Nucl. Phys. B370(1992)432; LNGS-91/01.

[6] MACRO Collaboration, S.Ahlen et al., "Study of the ultrahigh energy primary cosmic ray composition with the MACRO experiment", Phys. Rev. D46(1992)895.

[7] MACRO Collaboration, S.Ahlen et al., "Measurement of the decoherence function with the MACRO detector at Gran Sasso", Phys. Rev. D46(1992)4836; LNGS-92/29.

[8] MACRO Collaboration, S.Ahlen et al., "Search for neutrino bursts from collapsing stars with the MACRO detector", Astroparticle Phys. 1(1992)11; LNGS-92/32.

[9] MACRO Collaboration, S.Ahlen et al., "Search for nuclearites using the MACRO detector", Phys. Rev. Lett. 69(1992)1860.

[10] MACRO Collaboration, S.Ahlen et al., "First supermodule of the MACRO detector at Gran Sasso", Nucl. Inst. Meth. Phys. Res. A324(1993)337; LNGS 92/34.

[11] MACRO Collaboration, S.Ahlen et al., "Muon astronomy with the MACRO detector", Astrophys. J. 412(1993)301.

[12] MACRO Collaboration, S.Ahlen et al., "Search for slow moving magnetic monopoles with the MACRO detector", Phys. Rev. Lett. 72(1994)608; LNGS 93/84.

[13] GRACE-MACRO Collaborations, M.Ambrosio et al., "Coincident observation of air Cherenkov light by a surface array and muon bundles by a deep underground detector", Phys. Rev. D50(1994)3046.

[14] EASTOP-MACRO Collaborations, M.Aglietta et al., "Study of the primary cosmic ray composition around the knee of the energy spectrum", Phys. Lett. B337(1994)376.

[15] MACRO Collaboration, M.Ambrosio et al., "Performance of the MACRO streamer tube system in the search for magnetic monopoles", Astroparticle Phys. 4(1995)33; LNGS 95/11.

[16] MACRO Collaboration, M.Ambrosio et al., "Vertical muon intensity measured with MACRO at the Gran Sasso laboratory", Phys. Rev. D52(1995)3793.

[17] MACRO Collaboration, M.Ambrosio et al., "Atmospheric neutrino flux measurements using upgoing muons", Phys. Lett. B357(1995)481.

[18] MACRO Collaboration, M.Ambrosio et al., "The performance of MACRO liquid scintillator in the search for magnetic monopoles with $10^{-3} \leq \beta \leq 1$", Astroparticle Phys. 6(1997)113; INFN-AE 96/22.

[19] MACRO Collaboration, M.Ambrosio et al. "High energy cosmic ray physics with the MACRO detector at Gran Sasso: Part I. Analysis methods and experimental results", Phys. Rev. D56(1997)1407; INFN-AE 96/28.

[20] MACRO Collaboration, M.Ambrosio et al., "High energy cosmic ray physics with the MACRO detector at Gran Sasso: Part II. Primary spectra and composition", Phys. Rev. D56(1997)1418; INFN-AE 96/29.

[21] MACRO Collaboration, M.Ambrosio et al., "Seasonal variations in the underground muon intensity as seen by MACRO", Astroparticle Phys. 7(1997)109; INFN-AE 97/05.

[22] MACRO Collaboration, M.Ambrosio et al., "Magnetic monopole search with the MACRO detector at Gran Sasso", Phys. Lett. B406(1997)249; INFN-AE 97/16.

[23] MACRO Collaboration, M.Ambrosio et al. "Real time supernova neutrino burst detection with MACRO", Astroparticle Phys. 8(1998)123; INFN-AE 97/44.

[24] MACRO Collaboration, M.Ambrosio et al., "The observation of upgoing charged particles produced by high energy muons in underground detectors", Astroparticle Phys. 9(1998)105; INFN-AE 97/55; hep-ex/9807032.

[25] MACRO Collaboration, M.Ambrosio et al. "Measurement of the atmospheric neutrino-induced upgoing muon flux using MACRO", Phys. Lett. B434(1998)451; INFN-AE 98/13; hep-ex/9807005.

[26] MACRO Collaboration, M.Ambrosio et al., "Observation of the shadowing of cosmic rays by the Moon using a deep underground detector", Phys. Rev. D 59(1999)012003; INFN-AE 98/14; hep-ex/9807006.

[27] MACRO Collaboration, M.Ambrosio et al., "Measurement of the energy spectrum of underground muons at Gran Sasso with a transition radiation detector", Astroparticle Phys. 10(1999)11; INFN-AE 98/15; hep-ex/9807009.

[28] MACRO Collaboration, M.Ambrosio et al., "Limits on dark matter WIMPs using upward-going muons in the MACRO detector", Phys. Rev. D60(1999)082002; hep-ex/9812020.

[29] MACRO Collaboration, M.Ambrosio et al., "High statistics measurement of the underground muon pair separation at Gran Sasso", Phys. Rev. D60(1999)032001; hep-ex/9901027; INFN-AE 99/04 (1999).

[30] MACRO Collaboration, M.Ambrosio et al., "Nuclearite search with the MACRO detector at Gran Sasso", Eur. Phys. J. C13(2000)453; hep-ex/9904031.

[31] MACRO Collaboration, M.Ambrosio et al., "Low energy atmospheric muon neutrinos in MACRO", Phys. Lett. B478(2000)5; hep-ex/0001044.

[32] MACRO Collaboration, M. Ambrosio et al., "A search for lightly ionizing particles with the MACRO detector", Phys. Rev. D62(2000)052003; hep-ex/0002029.

[33] MACRO Collaboration, M. Ambrosio et al., "Neutrino astronomy with the MACRO detector" Astrophys. J. 546(2001)1038; astro-ph/0002492.

[34] MACRO Collaboration, M.Ambrosio et al., "Matter effects in upward-going muons and sterile neutrino oscillations", Phys. Lett. B517(2001)59; hep-ex/0106049.

[35] MACRO Collaboration, M.Ambrosio et al., "The MACRO detector at Gran Sasso", accepted for publication on NIM A.

[36] MACRO Collaboration, M.Ambrosio et al., "A combined analysis technique for the search for fast magnetic monopoles with the MACRO detector", hep-ex/0110083; accepted for publication on Astroparticle Physics.

[37] P. Bernardini, "Neutrino astronomy using upward-travelling muons in MACRO", Invited talk at "Very High Energy Phenomena in the Universe", XXXVI Rencontres de Moriond, Les Arcs (2001).

[38] D. Bakari for the MACRO Collaboration, "Estimate of the energy of upgoing muons with multiple Coulomb scattering", hep-ex/0105087, Proceedings of the NATO ARW on Cosmic Radiations: from Astronomy to Particle Physics, Oujda (Morocco), 21-23 March 2001.

[39] G. Battistoni for the MACRO Collaboration, "Neutrino induced upgoing muon energy estimation by multiple scattering with MACRO", Proceedings of the NATO ARW on Cosmic Radiations: from Astronomy to Particle Physics, Oujda (Morocco), 21-23 March 2001.

[40] M. Cozzi and L. Patrizii for the MACRO Collaboration, "Nuclear track detectors. Searches for magnetic monopoles and for nuclearites", Proceedings of the NATO ARW on Cosmic Radiations: from Astronomy to Particle Physics, Oujda (Morocco), 21-23 March 2001.

[41] H. Dekhissi for the MACRO Collaboration, "Muon astronomy with the underground detectors", Proceedings of the NATO ARW on Cosmic Radiations: from Astronomy to Particle Physics, Oujda (Morocco), 21-23 March 2001.

[42] M. Grassi for the MACRO Collaboration, "A search for gravitational stellar collapses", Proceedings of the NATO ARW on Cosmic Radiations: from Astronomy to Particle Physics, Oujda (Morocco), 21-23 March 2001.

[43] S. Kyriazopoulou for the MACRO Collaboration, "Search for slow magnetic monopoles with the MACRO scintillation detector", Proceedings of the NATO ARW on Cosmic Radiations: from Astronomy to Particle Physics, Oujda (Morocco), 21-23 March 2001.

[44] F. Maaroufi and A. Margiotta for the MACRO Collaboration, "Daily variation studies with the MACRO detector", Proceedings of the NATO ARW on Cosmic Radiations: from Astronomy to Particle Physics, Oujda (Morocco), 21-23 March 2001.

[45] T. Montaruli for the MACRO Collaboration, "High energy neutrino astronomy and WIMP search results", Proceedings of the NATO ARW on Cosmic Radiations: from Astronomy to Particle Physics, Oujda (Morocco), 21-23 March 2001.

[46] L. Perrone for the MACRO Collaboration, "Search for a diffuse neutrino flux from astrophysical sources", Proceedings of the NATO ARW on Cosmic Radiations: from Astronomy to Particle Physics, Oujda (Morocco), 21-23 March 2001.

[47] F. Ronga for the MACRO Collaboration, "Atmospheric neutrinos and neutrino oscillations in the MACRO experiment", Proceedings of the NATO ARW on Cosmic Radiations: from Astronomy to Particle Physics, Oujda (Morocco), 21-23 March 2001.

[48] M. Sitta for the MACRO Collaboration, "Monopole catalysis of nucleon decay: theory and experimental results", Proceedings of the NATO ARW on Cosmic Radiations: from Astronomy to Particle Physics, Oujda (Morocco), 21-23 March 2001.

[49] I. De Mitri for the MACRO Collaboration, "Search for magnetic monopoles in the cosmic radiation with the MACRO detector at Gran Sasso ", International Europhysics Conference on High Energy Physics, Budapest, July 12-18 2001.

[50] E. Scapparone et al. for the MACRO Collaboration, "Study of neutrino induced upgoing muon energy", International Europhysics Conference on High Energy Physics, Budapest, July 12-18 2001.

[51] G. Giacomelli and M. Giorgini for the MACRO Collaboration, "Atmospheric neutrino oscillations in MACRO", Invited talk at NO-VE, Intern. Workshop on Neutrino Oscillation in Venice, 24-26 July 2001

[52] F. Cei for the MACRO Collaboration, "Search for lightly ionizing particles with the MACRO detector", ICRC 2001, Hamburg, Germany, 7-15 August 2001.

[53] N. Giglietto for the MACRO Collaboration, "Moon and Sun shadowing effect on the MACRO apparatus", ICRC 2001, Hamburg, Germany, 7-15 August 2001.

[54] T. Montaruli for the MACRO Collaboration, "Final results on atmospheric neutrino oscillations with MACRO", ICRC 2001, Hamburg, Germany 7-15 August 2001.

[55] S. Mufson for the MACRO Collaboration, "Measurement of the Solar Diurnal and Sidereal Muon Waves with MACRO", ICRC 2001, Hamburg, Germany, 7-15 August 2001.

[56] L. Perrone for the MACRO Collaboration, "Neutrino astronomy with MACRO", ICRC 2001, Hamburg, Germany, 7-15 August 2001.

[57] M. Sioli for the MACRO Collaboration, "Measurement of the ratio double/single muon events as a function of rock depth with MACRO", hep-ex/0201017;"Use of Coulomb scattering for determining neutrino energies with MACRO", hep-ex/0201016, ICRC 2001, Hamburg, Germany, 7-15 August 2001.

[58] M. Sitta for the MACRO Collaboration, "Rare particle searches with MACRO", ICRC 2001, Hamburg, Germany, 7-15 August 2001.

[59] M. Spurio for the MACRO Collaboration, " Low energy atmospheric ν_μ measurements", ICRC 2001, Hamburg, Germany, 7-15 August 2001.

[60] P. Vallania for the EASTOP-MACRO Collaboration, "The primary CR composition around the knee from EAS e.m., GeV and TeV muon data", ICRC 2001, Hamburg, Germany, 7-15 August 2001.

[61] G. Battistoni for the MACRO Collaboration, "Cosmic ray composition around the knee from EAS electromagnetic and muon data", astro-ph/0112473; "Study of cosmic ray primaries and their cascade at $E_o = 10 - 100$ TeVthrough EAS-TOP and MACRO", astro-ph/0112475; TAUP 2001, Laboratori Nazionali del Gran Sasso, September 8-12 2001.

[62] I. De Mitri for the MACRO Collaboration, "Search for massive rare particles in MACRO", TAUP 2001, Laboratori Nazionali del Gran Sasso, September 8-12 2001.

[63] E. Scapparone for the MACRO Collaboration, "Study of neutrino induced upgoing muon energy with MACRO", TAUP 2001, LNGS, September 8-12, 2001.

[64] M. Giorgini for the MACRO Collaboration, "Performance of the MACRO limited streamer tubes for estimates of muon energies ", 7th Int. Conf. on Advanced Technology and Particle Physics, Como, Italy (2001).

[65] V. Agrawal et al., Phys. Rev. D53(1996)1314.

[66] M. Gluck et al., Z. Phys. C67(1995)433.

[67] W. Lohmann et al., "Energy loss of muons in the energy range 1 - 10000 GeV" CERN 85-03.

[68] G. Feldman and R. Cousins, Phys. Rev. D57(1998)3873.

[69] M. Giorgini, "Study of atmospheric neutrino oscillations by energy estimates of upgoing muons in MACRO", Tesi di Dottorato, Università di Bologna (2002).

[70] SuperKamiokande Coll., Y.Fukuda et al., Phys. Rev. Lett. 81(1998)1562; Phys. Lett. B433(1998)9; Phys. Rev. Lett. 85(2000)3999; Nucl. Phys. B Proc. Suppl. 91(2001)127; T. Toshito, hep-ex/0105023 (2001).

[71] Soudan 2 Coll., W.W.M. Allison et al., Phys. Lett. B391 (1997) 491; Phys. Lett. B449 (1999) 137; W. Anthony Mann, hep-ex/0007031 (2000); T. Mann et al., Nucl. Phys. B Proc. Suppl. 91 (2001) 134.

[72] P. Lipari et al., Phys. Rev. Lett. 74(1995)384.

[73] A. Bottino, N. Fornengo, F. Donato and S. Scopel (private communication). N. Fornengo, in Proceedings of the Ringberg Euroconference "New Trends in Neutrino Physics", Ringberg Castle, Tegernsee, Germany, 1998, edited by B. Kniel, World Scientific, Singapore.

[74] R. Bernabei et al., Phys. Lett. B389(1996)757.

[75] G. Giacomelli and L. Patrizii, "Magnetic monopoles", Lecture at the Fifth School on Particle Astrophysics, Trieste 29 June-10 July 1998, hep-ex/0002032.
G. Giacomelli et al. (Magnetic Monopole Bibliography) hep-ex/0005041.

[76] J. Derkaoui et al., Astropart. Phys. 9(1998)173; Astropart. Phys. 10(1999)339.

[77] S. Nakamura et al., Phys. Lett. B263(1991)529.

[78] S. Orito et al., Phys. Rev. Lett. 66(1991)1951.

[79] D. Bakari et al., "Magnetic monopoles, nuclearites, Q-balls: a qualitative picture", hep-ex/0004019.

[80] P. B. Price, Phys. Rev. D38(1988) 3813.

[81] D. Ghosh and S. Chatterjea, Europhys. Lett. 12(1990)25.

[82] M. Sioli, "A new approach to the study of high energy muon bundles with the MACRO detector at Gran Sasso", Tesi di Dottorato, Università di Bologna (2000).

[83] P. Lipa, P. Carruthers, H.C. Eggers and B. Buschbeck, Phys. Lett. 285B(1992)300.

[84] G. Battistoni et al., LNGS-95-09 (1995); Proceedings of the XXIV Int. Cosmic Ray Conf., Roma, 1995, ed. N. Iucci et al., Arti Grafiche Editoriali, Urbino, (1995), Vol. 1, p. 508.

[85] J. W. Elbert et al, XVII ICRC (Paris, 1981) Vol. 7, p.42.

[86] O. G. Ryazhskaya for the LVD Collaboration, Nucl. Phys. (Proc. Suppl.) B87(2000)423.

[87] P. Antonioli et al., Astrop. Phys. 7(1997)357.

[88] J.N. Capdevielle et al., KFK Report (1992)4998; FZKA (1998)6019.

[89] EAS-TOP Collaboration, M. Aglietta et al., Nucl. Phys. B54B(1997)263.

[90] J. Knapp and D. Heck, Extensive Air Shower Simulation with CORSIKA 5.61 (1998).

[91] M. Aglietta et al., Nucl. Instr. & Meth. A336(1993)310.

[92] EAS-TOP Coll., Astroparticle Physics, 10, 1, 1999 and Proc. 26th ICRC, 1, 230, (1999).

[93] S. Cecchini et al., "New calibrations and time stability of the INTERCAST CR-39", Radiat. Meas. 34(2001)55, hep-ex/0104022.